



# Water Quality Trends and Eutrophication Indicators in a Large Subtropical Estuary: A Case Study of the Greater Charlotte Harbor System in Southwest Florida

M. Medina<sup>1,2</sup> · M. W. Beck<sup>3</sup> · J. Hecker<sup>4</sup> · N. Iadevaia<sup>4</sup> · B. Moody<sup>5</sup> · C. Anastasiou<sup>6</sup> · D. Tomasko<sup>7</sup> · E. C. Milbrandt<sup>8</sup> · D. Kaplan<sup>2</sup> · C. Angelini<sup>2</sup>

Received: 30 April 2024 / Revised: 8 January 2025 / Accepted: 10 January 2025  
© The Author(s), under exclusive licence to Coastal and Estuarine Research Federation 2025

## Abstract

Tracking symptoms of eutrophication over time with multiple lines of evidence provides critical information to support environmental management and restoration efforts. For this case study of the Greater Charlotte Harbor estuary system in southwest Florida (USA), we assembled and curated 22 years of monthly water quality data from a spatially stratified random sampling design; estimated trends in annual mean concentrations of nitrogen, phosphorus, and chlorophyll-a across 13 monitoring strata over a sliding 5-year window between 2000 and 2021; identified hot spots where annual mean concentrations were increasing or elevated between 2017 and 2021, relative to stratum-specific thresholds informed by regulatory criteria; and summarized concurrent data from long-term surveys of macroalgal abundance and seagrass acreage. The water quality trend analysis methodology, based on generalized additive models (GAMs), captured seasonality and nonlinear inter-annual tendencies while accounting for uncertainty. Throughout the system, concentrations of total nitrogen increased and exceeded stratum-specific thresholds during the 2010 decade, while concentrations of total phosphorus and chlorophyll-a typically decreased to levels near or below thresholds. Low concentrations of inorganic nitrogen fractions indicated rapid biological assimilation consistent with eutrophication, while low chlorophyll-a concentrations indicated that nitrogen enrichment did not translate into excessive phytoplankton production. Instead, macroalgal proliferation and substantial seagrass losses were observed following Hurricane Irma (September 2017). We speculate that nitrogen enrichment during the 2010s increased the system's vulnerability to Irma's effects and helped tip the system toward these profound ecological changes. This work provides a broadly applicable framework for documenting and evaluating symptoms of eutrophication in estuaries.

**Keywords** National estuary programs · Nitrogen · Macroalgae · Seagrass · Coastal · Generalized additive models

## Introduction

Cultural eutrophication of coastal waters (i.e., increased primary production due to anthropogenic nutrient enrichment) contributes to degradation of water quality, excessive

---

Communicated by Michael Wetz

✉ M. Medina  
research@eccoscientific.com

- <sup>1</sup> ECCO Scientific LLC, St. Petersburg, FL, USA
- <sup>2</sup> Center for Coastal Solutions, Department of Environmental Engineering Sciences, University of Florida, Gainesville, FL, USA
- <sup>3</sup> Tampa Bay Estuary Program, St. Petersburg, FL, USA
- <sup>4</sup> Coastal & Heartland National Estuary Partnership, Port Charlotte, FL, USA

- <sup>5</sup> Charlotte County Board of County Commissioners, Port Charlotte, FL, USA
- <sup>6</sup> Southwest Florida Water Management District, Brooksville, FL, USA
- <sup>7</sup> Sarasota Bay Estuary Program, Sarasota, FL, USA
- <sup>8</sup> Marine Laboratory, Sanibel-Captiva Conservation Foundation, Sanibel, FL, USA

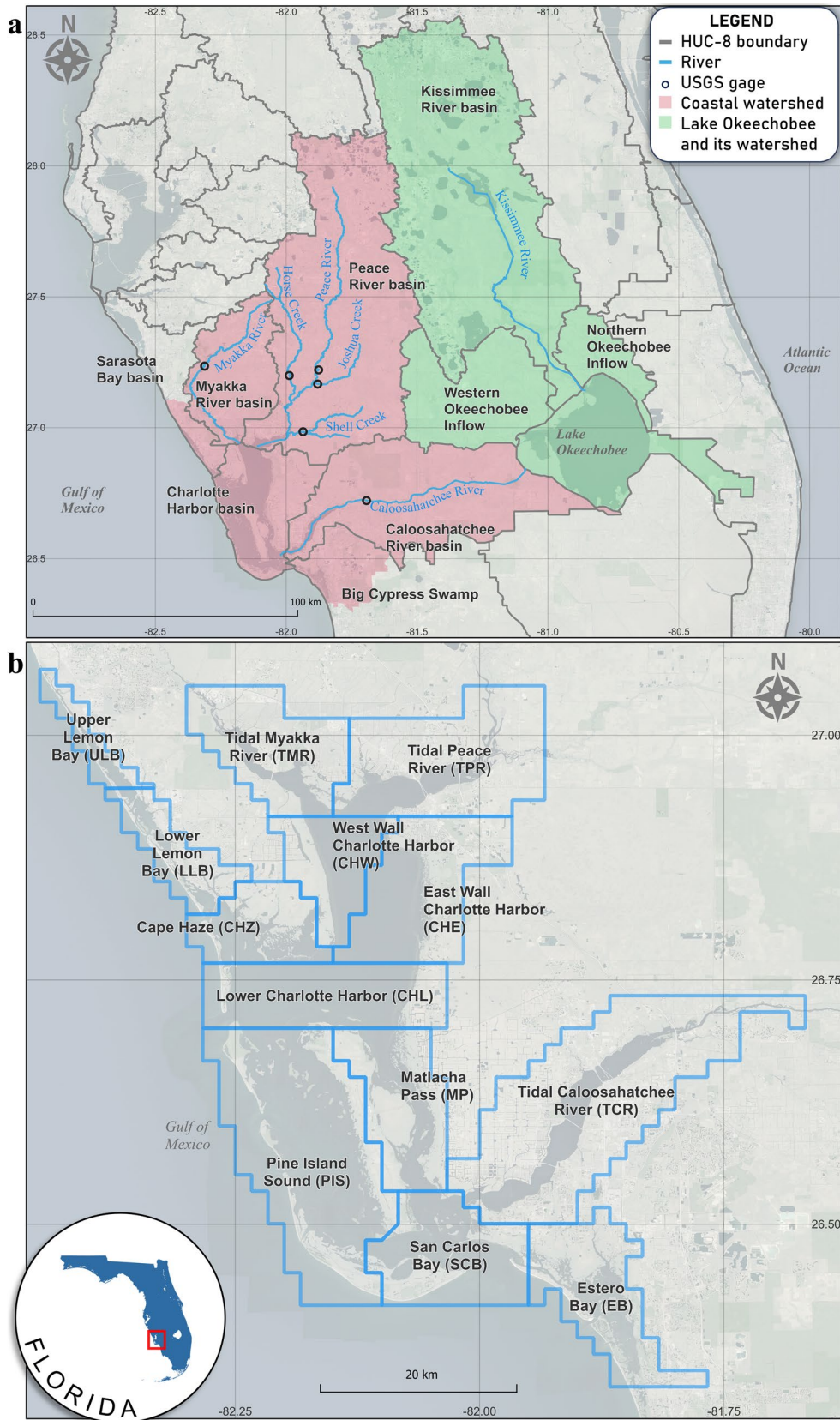


**Fig. 1** Study area. **a** The CCHMN area receives flows from coastal watersheds (red) and engineered discharges from Lake Okeechobee and its watershed (green) via the Caloosahatchee River. Gray boundaries indicate HUC-8 units. Black points mark the USGS gage locations used to calculate surface discharges in Fig. 2. **b** The CCHMN study area comprises 13 strata (blue boundaries)

growth of phytoplankton and macroalgae, harmful algal blooms, hypoxia, wildlife mortality, and loss of habitat and biodiversity (Anderson et al., 2021; Dunic et al., 2021; Orth et al., 2006; Paerl, 2009). Eutrophication is exacerbated by synergistic stressors that operate from local to global scales, including climate change and altered hydrologic regimes (Claussen et al., 2009; Dunic et al., 2021; Beck et al., 2023; Pannard et al., 2024). Claussen et al. (2009) frame eutrophication in terms of *causes*, including nutrient enrichment and physical factors such as temperature and hydrodynamics; *direct effects* such as production of phytoplankton and macroalgae; and *indirect effects* such as hypoxia, algal toxins, light attenuation, and habitat change.

Tracking and understanding eutrophication over time provides critical information for managing and restoring coastal ecosystems, assessing regulatory compliance, evaluating development plans, and placing the impacts of pulse disturbances in a historical context (Beck et al., 2022; Malone & Newton, 2020; Morrison et al., 2023; Schiff et al., 2016). Because eutrophication produces multiple system-specific structural and functional changes, it is useful to consider multiple indicators as lines of evidence when studying any system of interest (Cloern, 2001). Concentrations of nutrients, chlorophyll-*a* (as a proxy for phytoplankton abundance), and other water quality parameters commonly serve as primary indicators of eutrophication (Schiff et al., 2016). Complementary indicators of ecological effects include macroalgal abundance and seagrass coverage (e.g., Lapointe et al., 1994; Scolaro et al., 2023).

The Greater Charlotte Harbor estuary system in southwest Florida (USA) serves as a useful case study for understanding long-term changes in water quality and ecological indicators within a context of land use intensification and engineered hydrologic alteration (Fig. 1a). The system receives nutrient-enriched freshwater flows from a highly developed watershed via three major rivers—the Caloosahatchee, Peace, and Myakka—as well as smaller streams and canals that are directly connected to the coast. Inputs of freshwater and nitrogen loads to the system are dominated by the Caloosahatchee and Peace Rivers (Fig. 2; Tomasko et al., 2024), which integrate loads from highly urbanized coastal areas as well as inland agricultural and phosphate mining areas (Medina et al., 2022; Montefiore et al., 2024; Turner et al., 2006). Nitrogen loading from the Peace River basin increased approximately threefold between 1800 and 2000—based on an analysis of sediment cores—attributable

to population growth and land use development (Turner et al., 2006). To the south, construction of a canal connecting Lake Okeechobee to the Caloosahatchee River in the nineteenth century enables delivery of nutrient-enriched (and sometimes cyanobacteria-laden) discharges from the Lake to the coast via engineered flow control structures, artificially expanding the contributing watershed to include the Kissimmee River basin in central Florida (Medina et al., 2022; Pierce et al., 2004; Steinman et al., 2002). Nutrient loading to the Greater Charlotte Harbor estuary system has been linked to macroalgal blooms (Lapointe & Bedford, 2007; Milbrandt et al., 2019), hypoxic events (Milbrandt et al., 2021; Vargo, 2009), seagrass loss (Julian et al., 2024), and intensification of nearly annual *Karenia brevis* (red tide) blooms (Brand & Compton, 2007; Heil et al., 2014; Medina et al., 2020, 2022; Tomasko et al., 2024).

Understanding how cultural eutrophication unfolds in the coastal environment requires consistent monitoring effort, a reliable data management pipeline, and appropriate empirical methods capable of capturing nuances in the observed dynamics. Long-term monitoring efforts throughout the Greater Charlotte Harbor estuary system provide the opportunity to quantify and characterize eutrophication using multiple lines of evidence. For this study, we have (1) assembled and curated water quality data collected by the Coastal Charlotte Harbor Monitoring Network (CCHMN) according to a stratified random sampling design, to produce a robust 22-year dataset; (2) estimated trends in annual mean concentrations of nitrogen, phosphorus, and chlorophyll-*a* across 13 monitoring strata between 2000 and 2021; (3) identified water quality hot spots where annual mean concentrations were elevated and/or increasing relative to stratum-specific thresholds between 2017 and 2021; and (4) summarized data from annual macroalgae transects and biennial seagrass surveys. The water quality trend analyses were performed on a sliding 5-year window (between 2000 and 2021) using a statistical framework that captures seasonality and nonlinear trends while accounting for uncertainty (Beck et al., 2022). Trends and hot spots for 2017–2021 were interpreted in the context of Hurricane Irma (September 2017) and subsequent macroalgal proliferation and seagrass losses observed throughout the system (Garcia et al., 2020; Tomasko et al., 2018, 2020).

This study provides a generalizable framework for translating long-term monitoring data from coastal systems into a detailed history describing how symptoms of eutrophication have evolved over time, to inform ecological management and restoration plans. The indicators examined in this study provide a broad assessment of eutrophication in the Greater Charlotte Harbor estuary system, borrowing from the three interdependent categories of Claussen et al. (2009): causes (nutrient concentrations), direct effects (chlorophyll-*a* concentrations and macroalgal abundance), and indirect effects

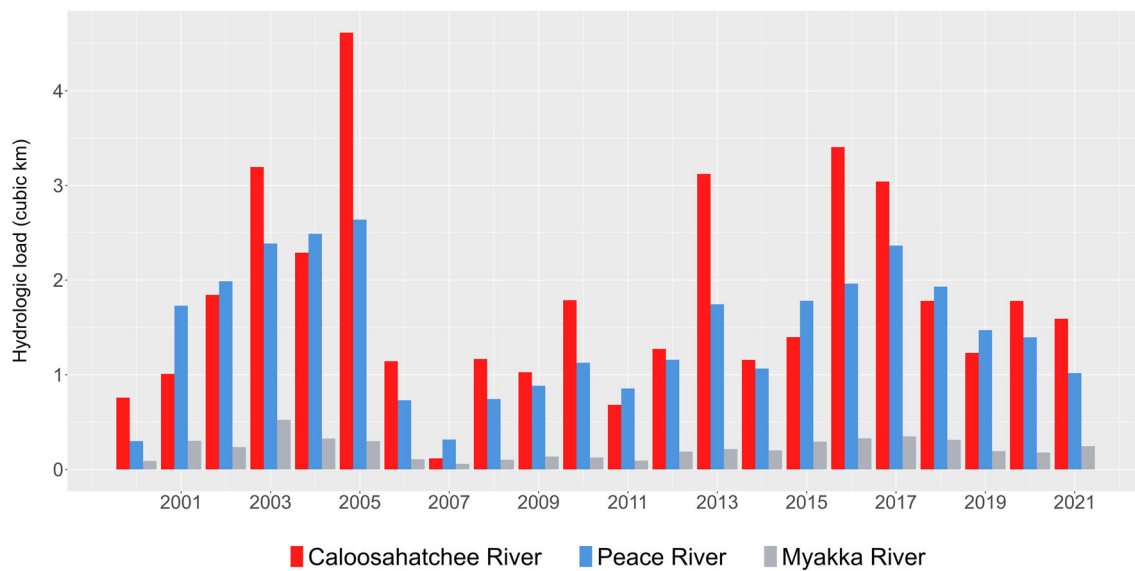


**Fig. 2** Annual riverine discharges measured at the Caloosahatchee River at S-79, in red (USGS gage 02292900); Peace River at Arcadia, Horse Creek, Joshua Creek and Shell Creek, in blue (02296750, 02297310, 02297100, and 02298202, respectively); and Myakka

River, in gray (02298830). These gages do not represent the full watershed contributing surface water flows to the CCHMN study area (see Fig. 1a)

(seagrass coverage). Informed by prior studies documenting eutrophication symptoms throughout the Greater Charlotte Harbor system (e.g., Garcia et al., 2020; Tomasko et al., 2020) and other subtropical systems (e.g., Burkholder et al., 2007; Teichberg et al., 2010), we hypothesized that nutrient increases throughout the system manifested primarily as changes in macroalgal and seagrass abundance rather than phytoplankton production.

## Methods

### Study Area

The Greater Charlotte Harbor estuary system in southwest Florida spans more than 700 km<sup>2</sup> of diverse coastal and submerged habitats including mangroves, salt marshes, tidal flats, and seagrass meadows (Duffrey et al., 2007). Seagrass communities include *Halodule wrightii*, *Thalassia testudinum*, *Syringodium filiforme*, and other species within the shallower regions of each segment, ranging from depths of 0.8 m in the Tidal Peace River to 2.2 m in San Carlos Bay (Corbett & Hale, 2006; Tomasko et al., 2018, 2020; Garcia et al., 2020). This shallow subtropical estuary system comprises three tidal river estuaries (Caloosahatchee, Peace, and Myakka) and associated bays (Fig. 1a).

For purposes of environmental monitoring and scientific study, the Greater Charlotte Harbor estuary system is commonly divided into 13 segments (Fig. 1b) (CHNEP, 2004; Corbett & Hale, 2006; CHNEP, 2019). The interaction of

riverine discharges and tidal cycles over the complex geomorphology and benthic habitats of this large estuarine system generates complex hydrodynamics that connect the northern and southern segments (Dye et al., 2020; Hewageegana et al., 2023; Shi et al., 2023). Northern segments of Charlotte Harbor (in particular, the East Wall and West Wall) are heavily influenced by discharges from the Peace River as well as the Caloosahatchee River during periods of high discharge, via Matlacha Pass (Dye et al., 2020; Hewageegana et al., 2023; Shi et al., 2023). Due to its lack of direct connectivity to the Gulf of Mexico, Matlacha Pass generally experiences longer residence times and poorer water quality than the adjacent San Carlos Bay, especially during periods of low discharge from the Caloosahatchee River (Hewageegana et al., 2023), whereas Lower Charlotte Harbor, Cape Haze, and Pine Island Sound are typically dominated by non-colored water from the Gulf of Mexico (McPherson et al., 1996). Salinity gradients extend along river channels during periods of low discharge, whereas high discharges induce lower salinities and vertical density stratification (McPherson et al., 1996; Shi et al., 2023; Turner et al., 2006). Nutrient and chlorophyll-a gradients generally extend from tidal river segments toward the Gulf of Mexico (McPherson et al., 1996; Turner et al., 2006).

Several hydrologic units (HUC-8) drain directly into the system, including the Charlotte Harbor basin; the Caloosahatchee, Peace, and Myakka River basins; and parts of the Sarasota Bay and Big Cypress Swamp units (Fig. 1a). Discharges from the Caloosahatchee River are released at the S-79 flow control structure operated by the U.S. Army Corps

of Engineers. In addition to flows originating within its basin (both upstream and downstream of the S-79 structure), the Caloosahatchee River receives engineered flows from Lake Okeechobee via the S-77 structure (Montefiore et al., 2024; Rumbold & Doering, 2020). Hydrologic and nitrogen loads into the eutrophic Lake are dominated by inputs from the Kissimmee River basin (Ma et al., 2020). Lake discharges are also released south to the Florida Everglades and east to the Atlantic coast via the St. Lucie River through a highly engineered system of canals and flow control structures. Flows from the Peace and Myakka Rivers and their tributaries into Charlotte Harbor are virtually unregulated aside from a few passive weir structures (McPherson et al., 1996; SWFWMD, 2010).

Surface discharges measured at USGS gage stations on the Caloosahatchee River, Peace River (and three main tributaries: Horse Creek, Joshua Creek, and Shell Creek), and Myakka River are visualized in Fig. 2 to provide historical context, although these gages do not represent the full watershed contributing surface water flows to the study area (see gage locations in Fig. 1a). Drought conditions categorized as severe, extreme, or exceptional by the U.S. Drought Monitor (D2–D4 categories) occurred in parts of the watershed in 2000, 2001, 2007, 2008, 2009, 2011, 2012, and 2017 (NDMC, 2024). During the study period, hurricanes made landfall in southwest Florida in August and September 2004 (Charley, Frances, and Jeanne) and September 2017 (Irma) (Tomasko et al., 2006, 2020).

In 2012, the State of Florida adopted segment-specific quantitative nutrient criteria for concentrations of total nitrogen, total phosphorus, and chlorophyll-*a* in the water column (Florida Administrative Code 62–302.531). Development of these water quality criteria was motivated by seagrass losses in other southern Florida estuaries during the latter half of the twentieth century and aimed to maintain water clarity consistent with seagrass conservation (Corbett & Hale, 2006). The spatial specificity of the criteria reflects variability in nutrient effects moderated by residence time, light penetration, and other considerations that vary across segments (Garcia et al., 2020).

## Curation of Water Quality Data

The CCHMN monitors water quality along a section of the southwest Florida coast extending from Estero Bay in the south to Lemon Bay in the north, including Charlotte Harbor and the tidal segments of the Peace, Myakka, and Caloosahatchee Rivers (Fig. 1a). Monitoring follows a geographically stratified random sampling design across 13 “strata” (Fig. 1b) that are considered relatively homogeneous in terms of water quality and habitat conditions (CHNEP, 2004; 2019). Each month, grab samples and sonde measurements are collected at five random locations within each of the 13 strata following standardized procedures for measurement, collection, and chemical analysis (CHNEP, 2004; CHNEP, 2019; CHNEP, 2023). Collectively, we refer to the entire study area as “Greater Charlotte Harbor,” and we refer to the West Wall, East Wall, Lower Charlotte Harbor, and Cape Haze strata as “Charlotte Harbor proper.” As a regional partnership coordinated by the Coastal & Heartland National Estuary Partnership (CHNEP), the CCHMN includes Charlotte County, Florida; City of Cape Coral, Florida; Lee County, Florida; Sarasota County, Florida; Southwest Florida Water Management District (SWFWMD); Florida Fish & Wildlife Conservation Commission (FWC); and Florida Department of Environmental Protection (FDEP).

Data collected by the CCHMN include water quality parameters listed in Table 1 as well as dissolved oxygen, biological oxygen demand, total organic carbon, apparent color, pH, Secchi disk depth, salinity, specific conductance, temperature, and bacteria. Despite standardization of sampling and lab protocols, the CCHMN data were distributed across several public databases using different data labeling conventions and therefore had to be assembled and curated to support this work. To facilitate future research and reproducibility of the analyses herein, the curated CCHMN dataset is provided as original open-source material in Medina (2024). This study relies on nitrogen, phosphorus, and chlorophyll-*a* concentration data from this curated dataset to quantify long-term trends between 2000 and 2021. Other parameters that are relevant to understanding eutrophication, such as

**Table 1** Water quality parameters

Abbreviation	Water quality parameter	Unit	<i>N</i> (all strata)	MDL range	Non-detection rate
Chlorophyll- <i>a</i>	Chlorophyll- <i>a</i>	ug/L	22,753	0.01–5	5.9%
NHx-N	Ammonia nitrogen	mg/L	16,242	0.004–0.1	56.6%
NOx-N	Nitrite + nitrate nitrogen	mg/L	24,379	0.004–0.05	44.0%
TKN	Total Kjeldahl nitrogen	mg/L	23,643	0.01–0.25	3.1%
TN	Total nitrogen	mg/L	26,072	0.01–0.25	1.3%
PO4-P	Orthophosphate phosphorus	mg/L	23,696	0.002–0.2	21.8%
TP	Total phosphorus	mg/L	23,253	0.002–0.2	4.5%

dissolved oxygen and apparent color, were excluded from the study because they fluctuate on shorter timescales than the monthly sampling frequency of the CCHMN data or because consistent long-term data were not available across the system.

The CCHMN data for the period January 2000 through December 2021 were assembled by acquiring data from (1) FDEP Watershed Information Network (WIN) and its archived predecessor, STORET; (2) SWFWMD Environmental Data Portal; and (3) CHNEP Water Atlas (Table 1). The latter two sources routinely submit data for inclusion in WIN/STORET, and SWFWMD submits some data for inclusion in the CHNEP Water Atlas. The data were compiled preferentially in the above-specified order—i.e., gaps in the WIN/STORET record were filled with data from SWFWMD first, and remaining gaps were filled with data from CHNEP Water Atlas. We applied rigorous data cleaning procedures to standardize data labels (analyte names, stratum names, and measurement units), standardize reported values for non-detect samples (reported at the method detection limit, as described below), remove duplicate records, and remove records flagged with fatal qualifier codes or with physically impossible reported values.

Non-detects were reported at the method detection limit (MDL) consistent with FDEP protocols. Reporting the MDL value when a constituent is not detected is considered adequate when the non-detection rate is below 25%, although reporting another value, such as one-half of the MDL, may be preferable (Croghan & Egeghy, 2003). MDL values varied across strata and over time throughout the study period, and MDL values associated with non-detect samples are summarized in Table 1, visualized in histograms (Figure S1), and labeled in the curated dataset (Medina, 2024). Because the dataset includes a large number of records reporting non-detection of  $\text{NH}_x\text{-N}$ ,  $\text{NO}_x\text{-N}$ , and  $\text{PO}_4\text{-P}$  (see Table 1 for per-parameter non-detection rates aggregated across strata), we excluded these parameters from the trend analysis. Fewer non-detects were present in the TN, TKN, TP, and chlorophyll-*a* data ( $\leq 17\%$  at any given stratum).

Finally, we estimated the concentrations of unreported nitrogen fractions when the appropriate concentration values were reported from selfsame samples (identified by sample location, depth, date, and time), according to the arithmetic relations  $\text{NO}_x = \text{NO}_2 + \text{NO}_3$  and  $\text{TN} = \text{TKN} + \text{NO}_x$ . Calculated (unreported) nitrogen values were relatively rare, representing 8.6% of TN records (including all TN data for Upper Lemon Bay, or 8.3%), 0.9% of TKN records, and 3.6% of  $\text{NO}_x\text{-N}$  records. We developed internally consistent procedures for these calculations when one or more reported nitrogen fractions were not detected. Assuming the MDL for non-detects (as we did throughout the dataset) effectively means that we assume the maximum possible concentration in the sample. Using this idea as the guiding principle, we

developed rules for calculating unreported nitrogen fractions in the presence of non-detects. For example, when  $\text{NO}_2\text{-N}$  and  $\text{NO}_3\text{-N}$  were not detected, we added their MDLs to obtain the maximum possible concentration for  $\text{NO}_x\text{-N}$ . Or, if TKN was detected and  $\text{NO}_x\text{-N}$  was not detected, we calculated TN by adding the detected TKN concentration and the  $\text{NO}_x\text{-N}$  MDL. Calculations involving subtraction may initially seem counterintuitive. For example, to calculate TKN from detected TN and non-detected  $\text{NO}_x\text{-N}$ , we assume zero  $\text{NO}_x\text{-N}$  and adopt the detected TN concentration as the TKN concentration, to obtain the maximum possible TKN value, consistent with the guiding principle. Finally, calculations that resulted in negative concentration values were not included in the dataset (whether or not they involved non-detects). For example, a TKN value calculated as the difference between a TN concentration (e.g., 0.03 mg/L) and a larger  $\text{NO}_x\text{-N}$  concentration (e.g., 0.05 mg/L) would be abandoned.

The CCHMN data represent grab samples collected from the upper 1 m of the water column and do not account for constituents stored in the middle and lower water column or in bottom sediments. The data may nonetheless be considered reasonably representative of the water column considering the system's shallow depth, which averages less than 3 m (Montgomery et al., 1991; NOAA 2015). Vertical salinity stratification is relatively rare, occurring primarily within the tidal river segments during periods of high discharge (Montgomery et al., 1991; Turner et al., 2006; Kim et al. 2010; Shi et al., 2023), and the system is typically well-mixed in the shallower areas where seagrass and macroalgae are observed. Surface sampling is common practice in academic studies, monitoring programs, and regulatory assessments throughout the southwest Florida coast (Lapointe et al., 1994; McPherson et al., 1996; Montgomery et al., 1991; Tomasko et al., 2006, 2018, 2020).

## Water Quality Trend Analysis

Our analysis of water quality trends follows the framework introduced by Beck et al. (2022) based on generalized additive models (GAMs), a flexible form of regression that models a response variable using smooth functions of explanatory variables (Hastie & Tibshirani, 1986), and mixed-effects modeling to evaluate trends in seasonal metrics derived from the GAMs (Sera et al., 2019). This approach offers several advantages over other commonly used methods of trend analysis, including the flexibility to model seasonality and nonlinear inter-annual trends, robustness to data gaps and inconsistent sampling coverage, and propagation of uncertainty throughout the analysis (Beck et al., 2022; Sera et al., 2019). As a point of contrast, the non-parametric Seasonal Kendall test detects monotonic long-term changes with an adjustment for seasonal cycles, but the test imposes

assumptions that are often unrealistic in practice: that data are consistently sampled at a regular frequency without gaps, seasonal cycles are stationary, and inter-annual dynamics trend in a consistent direction (Hirsch et al., 1982). We refer the reader to Beck et al. (2022) for a fuller comparison of the GAM-based method with common alternatives.

For each water quality parameter at each stratum, the trend analysis proceeded in three steps, following Beck et al. (2022): (1) fit a generalized additive model (GAM) to the monthly mean concentrations over the full period of record (e.g., 2000–2021); (2) use the GAM fit to estimate annual mean values with 95% confidence intervals; and (3) estimate trends in the annual means over a sliding, right-justified 5-year window (e.g., 2000–2004, 2001–2005, ..., 2017–2021) using mixed-effects models that account for uncertainty in the annual means (Sera et al., 2019). Because nitrogen, phosphorus, and chlorophyll-a concentrations are typically lognormally distributed, the data were  $\log_{10}$ -transformed prior to analysis, and results were back-transformed to the linear scale.

The GAM estimates the water quality response (e.g., TN concentrations) using a smooth function of the decimal date (e.g., July 1, 2000, is represented as 2000.5) as the sole explanatory variable:

$$\hat{y} = \beta_0 + f_1(\text{date})$$

where  $\hat{y}$  is the estimate for the response variable of interest,  $\beta_0$  is the intercept, *date* is the decimal date, and  $f_1()$  is a smoothing spline (thin-plate spline) composed of the sum of the products of multiple basis functions and their coefficients (Beck et al., 2022). A large number of knots in the smooth term and the generalized cross-validation (GCV) fitting procedure provide sufficient flexibility to capture intra- and inter-annual variability while avoiding overfitting (Hastie & Tibshirani, 1986; Wood, 2017). Goodness of fit ( $R^2$ ) was not used as a basis for accepting or rejecting models, because the greater uncertainty associated with a poorly fitting GAM will translate into higher uncertainty in the mixed-effects model. It is appropriate for high variance in the data, especially from large outliers, to limit confidence in a trend assessment.

The GAM fit is then used to extract an estimated annual mean for the water quality response for each year in the period of record (other summary statistics such as the maximum or variance can be estimated, although we focused on the mean). Uncertainty in the annual mean is carried forward through subsequent steps of the procedure to estimate the trends in each 5-year window. Confidence intervals around annual mean estimates may reflect variability in the data and variability in sampling effort over time, and annual means with larger confidence intervals ultimately exert less influence on the slope of the trend line estimated by the

mixed-effects model. The mixed-effects model is essentially a linear regression with an additional random effect term that captures uncertainty in the estimated means:

$$\hat{\mu}_t = \beta_0 + \beta_1 t + b_t$$

where  $\hat{\mu}_t$  is the estimated mean for year  $t$ ,  $\beta_0$  is the intercept,  $\beta_1$  is the slope for year  $t$ , and  $b_t$  is the random effect for year  $t$  accounting for the uncertainty in the annual means from the GAM—i.e., the standard error of the mean (Beck et al., 2022; Sera et al., 2019). Trend slopes estimated over each 5-year window are reported in terms of the right-hand side of the window—for instance, the slope reported for 2021 corresponds to the 5-year window 2017–2021.

Trend results may be sensitive to the choice of window length: shorter window lengths provide less statistical power and are thereby less likely to detect meaningful trends, whereas longer window lengths are more likely to overgeneralize trends that change direction within shorter time periods. Our choice of the 5-year sliding window provides a reasonable balance capable of detecting meaningful inter-annual changes in the trend direction. Further, in practical terms, 5 years is a reasonable period over which management decisions and their outcomes can be evaluated.

## Water Quality Thresholds and Hot Spots

Florida Administrative Code (FAC) 62–302.532 specifies regulatory criteria for TN, TP, and chlorophyll-a concentrations at estuary segments whose boundaries roughly correspond to CCHMN strata, with the exception of Charlotte Harbor proper, which comprises four CCHMN strata (Table 2). We adopted these criteria values as thresholds for classifying annual mean concentrations of TN, TKN (TN criterion), TP, and chlorophyll-a at each stratum. Because FAC does not specify a numeric criterion for TN at Caloosahatchee River Estuary segments, we adopted the total maximum daily load (TMDL) target concentration for the lower tidal segment (Caloosahatchee Estuary, Tidal Segment 1) as the threshold for this stratum (FDEP, 2022). Each annual mean was classified as “above threshold” when the lower bound of the 95% confidence interval of the mean concentration exceeded the threshold; “below threshold” when the upper bound of the confidence interval was below the threshold; or “near threshold” if the confidence interval encompassed the threshold. Although the selection of concentration thresholds (Table 2) was informed by regulatory criteria, the results should not be interpreted as a regulatory assessment. Determination of regulatory impairments involves consideration of conditions on a finer spatial scale (compared to the scale of CCHMN strata) across multiple years (e.g., FDEP, 2022).

**Table 2** Stratum-specific concentration thresholds

CCHMN stratum	TN (mg/L)	TP (mg/L)	Chlorophyll-a (ug/L)
Tidal Peace River	1.08	0.50	12.6
Tidal Myakka River	1.02	0.31	11.7
West Wall, East Wall, Lower Charlotte Harbor, Cape Haze <sup>1</sup>	0.67	0.19	6.1
Upper Lemon Bay	0.56	0.26	8.9
Lower Lemon Bay	0.62	0.17	6.1
Tidal Caloosahatchee River <sup>2</sup>	0.45	0.04	5.6
Matlacha Pass	0.58	0.08	6.1
Pine Island Sound	0.57	0.06	6.5
San Carlos Bay	0.44	0.045	3.7
Estero Bay	0.63	0.07	5.9

Thresholds are adopted from segment-specific criteria in Florida Administrative Code (FAC) 62–302.532, unless otherwise specified

<sup>1</sup>FAC 62–302.532 specifies one set of numerical criteria for Charlotte Harbor proper, which comprises these four strata

<sup>2</sup>The TN threshold is adopted from the TMDL target concentration for the lower segment of the Caloosahatchee Estuary (Tidal Segment 1), per FDEP (2022). The TP and chlorophyll-a thresholds are adopted from the Lower Caloosahatchee River segment, per numeric criteria in FAC 62–302.532

Finally, we identified hot spots for nitrogen, phosphorus, and chlorophyll-a considering both the trend results for 2017–2021 and the threshold categories for 2021. A hot spot is defined as a stratum where the 2021 mean concentration exceeded the corresponding threshold and the 2017–2021 annual mean concentrations exhibited an upward trend or no trend—i.e., concentrations were consistently elevated, or elevated and increasing.

### Seagrass and Macroalgae Data

Starting in 1988, the SWFWMD has mapped areal seagrass coverage along Florida’s southwest coast in collaboration with regional partners—including Florida’s Aquatic Preserves, Florida Fish and Wildlife Conservation Commission, CHNEP, and other National Estuary Programs—with biennial maps available since 2002 (e.g., SWFWMD, 2019; SWFWMD, 2021; SWFWMD, 2023). The SWFWMD seagrass mapping area includes the Tidal Peace River, Tidal Myakka River, Charlotte Harbor proper (i.e., East Wall, West Wall, Lower Charlotte Harbor, and Cape Haze), and Upper and Lower Lemon Bay (Fig. 1b). The South Florida Water Management District (SFWMD) mapped seagrass in the southern strata (Pine Island Sound, Matlacha Pass, Tidal Caloosahatchee River, San Carlos Bay, and Estero Bay) less often, in 1999, 2003, 2004, 2008, 2014, and 2021 (SFWMD, 2001; SFWMD, 2004; SFWMD, 2006; SFWMD,

2009; SFWMD, 2015; SFWMD, 2022). In addition, the seagrass maps delineate “attached algae” areas dominated by macroalgal species (often *Caulerpa* spp.). Detached “drift” macroalgae are not mapped but are documented in field data and videos.

Seagrass mapping relies on aerial imagery acquired from an altitude of approximately 2400–3000 m under specified environmental conditions, photointerpretation based on photographic signatures with field verification, and independent third-party accuracy assessment for quality control (Garcia et al., 2020; Tomasko et al., 2005). For SWFWMD seagrass maps dated 1988 through 2020, the flight window for image acquisition was November through February (e.g., the 2020 map is based on imagery acquired between November 2019 and February 2020). Starting with the 2022 seagrass map, the flight window was changed to December through February due to changes in environmental conditions related to warming temperatures.

Drift macroalgae has been monitored annually since 1998 by the Charlotte Harbor Aquatic Preserves (CHAP) and Estero Bay Aquatic Preserve, administered by FDEP (FDEP & CHAP, 2024). The data are collected using one-square-meter quadrats spaced at regular intervals along transects that are grouped into strata roughly corresponding to the CCHMN strata boundaries, with two exceptions: (1) The “Lemon Bay” stratum comprises transect locations within the CCHMN strata of Upper Lemon Bay and Lower Lemon Bay and (2) Transects within the CCHMN stratum of Lower Charlotte Harbor are assigned to adjacent strata (FDEP, 2019)—see the map in supplementary Figure S2 for macroalgae transect locations. Macroalgal abundance is reported using Braun-Blanquet (BB) coverage classes: 0.1 (solitary individual), 0.5 (few individuals), 1 (<5% cover), 2 (5–25% cover), 3 (26–50% cover), 4 (51–75% cover), 5 (76–100% cover). For visualization, we aggregated the BB scores from each year’s macroalgae growing season (July through December) into evenly spaced coverage classes: 0% cover, 1–25% cover, 26–50% cover, 51–75% cover, and 76–100% cover. We also applied non-parametric one-sided Mann-Whitney tests for increases and decreases in macroalgal coverage between the pre- and post-Hurricane Irma periods (2014–2017 and 2018–2021).

### Code

Analyses were performed in R version 4.3.1 (R Core Team, 2023) using the following R packages: *wqtrends* (Beck et al., 2022), *mgcv* (Wood, 2011, 2017), *mixmeta* (Sera et al., 2019), *lubridate* (Grolemund & Wickham, 2011), *dplyr* (Wickham et al., 2023), and *plyr* (Wickham, 2011). R code that reproduces the water quality trend results is shared as open-source material at [https://github.com/milesmedina/CCHMN\\_trends\\_2021/](https://github.com/milesmedina/CCHMN_trends_2021/).

### Results

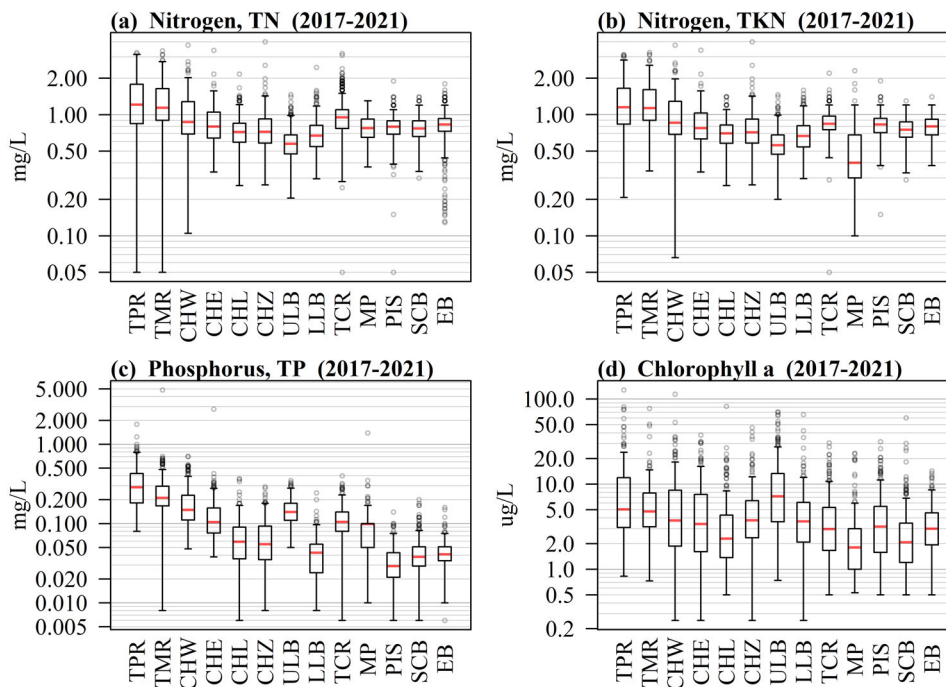
The distributions of nitrogen, phosphorus, and chlorophyll-a concentration data across strata during 2017–2021 provide a high-level perspective of water quality conditions during the final 5-year window of the study period (Fig. 3). Tidal river segments exhibited greater median concentrations of nutrients (TN, TKN, and TP) than their respective neighboring strata, and median chlorophyll-a concentrations were  $\leq 5$  ug/L (except for Upper Lemon Bay). Similar distributions of monthly averaged TKN and TN concentrations at each stratum suggest large TKN:TN ratios, except for Matlacha Pass where the median TKN concentration was noticeably lower than the median TN concentration. Additional visualizations of the water quality data, including data for inorganic nutrients and other parameters, are available at [https://github.com/milesmedina/CCHMN\\_trends\\_2021](https://github.com/milesmedina/CCHMN_trends_2021).

Inter- and intra-annual variability in the dynamics of TN, TKN, TP, and chlorophyll-a concentrations was captured by the GAMs (inorganic nutrients were excluded from trend analysis due to large numbers of non-detects), and the data generally exhibited expected seasonal patterns, with high concentrations observed during the summer wet season and/or early fall and lows during the dry

season. Annual mean concentrations estimated from the GAMs were then used to estimate trends with mixed-effects models. Figure 4 presents results for selected strata, and results for all 13 strata are presented in Figure S3. Fit statistics for the GAMs, including  $R^2$  and GCV scores, are included as supplemental material (GAM\_fit\_stats.csv).

The slopes of trends estimated over a sliding 5-year window (i.e., 2000–2004, 2001–2005, ..., 2017–2021) illustrate how 5-year trends have evolved over time, and these results are paired with categorization of the annual mean concentrations relative to the stratum-specific thresholds listed in Table 2 (Fig. 5). During the 2010 decade, annual mean TN concentrations were generally elevated relative to specified thresholds and exhibited many upward trends throughout the Greater Charlotte Harbor system. Several strata qualified as nitrogen hot spots during the 2017–2021 period—i.e., where TN concentrations were consistently elevated (Fig. 6). In contrast, annual mean concentrations of TP and chlorophyll-a were generally below or near specified thresholds. As noted in the “Methods” section, comparisons of annual mean concentrations to thresholds should not be interpreted as a regulatory assessment, even though the threshold values are based on regulatory criteria.

**Fig. 3** Distributions of nitrogen, phosphorus, and chlorophyll-a concentrations at each stratum during the final 5-year window in the study period (2017–2021). Boxplots display the median (red line); interquartile range, IQR (box);  $Q3 + 1.5 \cdot IQR$  and  $Q1 - 1.5 \cdot IQR$  (whiskers); and outliers (gray circles)



<b>TPR</b>	Tidal Peace River	<b>CHZ</b>	Cape Haze	<b>PIS</b>	Pine Island Sound
<b>TMR</b>	Tidal Myakka River	<b>ULB</b>	Upper Lemon Bay	<b>SCB</b>	San Carlos Bay
<b>CHW</b>	West Wall Charlotte Harbor	<b>LLB</b>	Lower Lemon Bay	<b>EB</b>	Estero Bay
<b>CHE</b>	East Wall Charlotte Harbor	<b>TCR</b>	Tidal Caloosahatchee River		
<b>CHL</b>	Lower Charlotte Harbor	<b>MP</b>	Matlacha Pass		

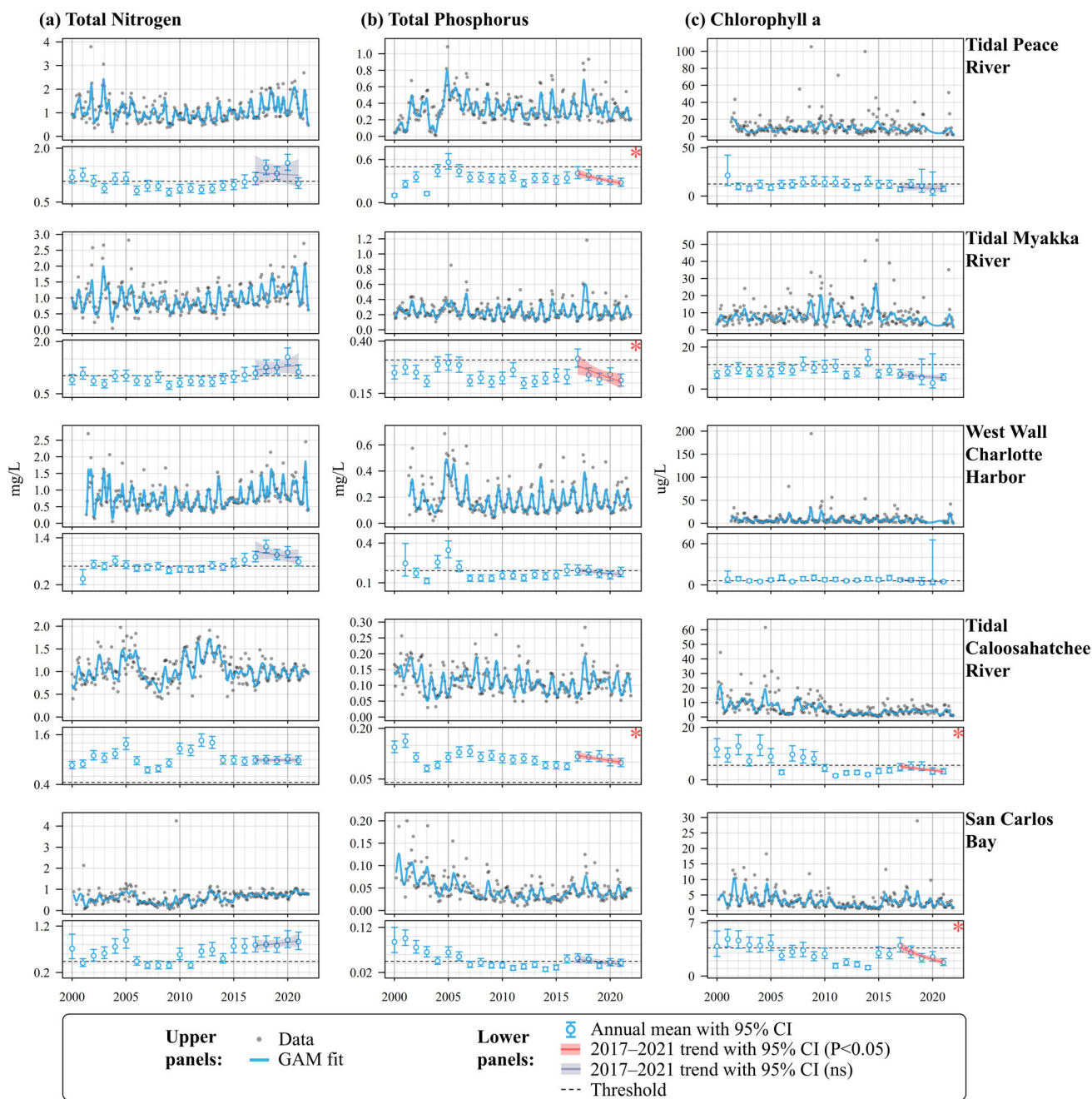


**Fig. 4** Trend results for concentrations of **a** total nitrogen, **b** total phosphorus, and **c** chlorophyll-a at selected CCHMN strata. The upper panels in each pair display concentration data (gray points) and GAM fits (blue curves). Lower panels display annual means with 95% confidence intervals (blue), stratum-specific thresholds (dotted

lines), and trends over the 2017–2021 window. Trends with statistically significant slopes ( $P < 0.05$ ) are colored red and marked with an asterisk; non-significant trends are colored gray. Figure S3 displays results for all 13 strata

### Nitrogen

Annual mean TN concentrations in the upper 1 m of the water column of the upper Harbor (Tidal Peace River, Tidal Myakka River, East Wall, West Wall, and Cape Haze) exhibited no 5-year trends during the first half of the study period (Fig. 5a). More recently, upward trends

appeared during five of the six 5-year windows terminating between 2015 and 2020 at each of these strata, except for Cape Haze, which exhibited upward trends during the 5-year windows terminating in 2017, 2018, and 2019. Annual mean TN concentrations at the East Wall, West Wall, and Cape Haze ranged between 0.6 mg/L and 1.2 mg/L between 2017 and 2021. Annual mean TN

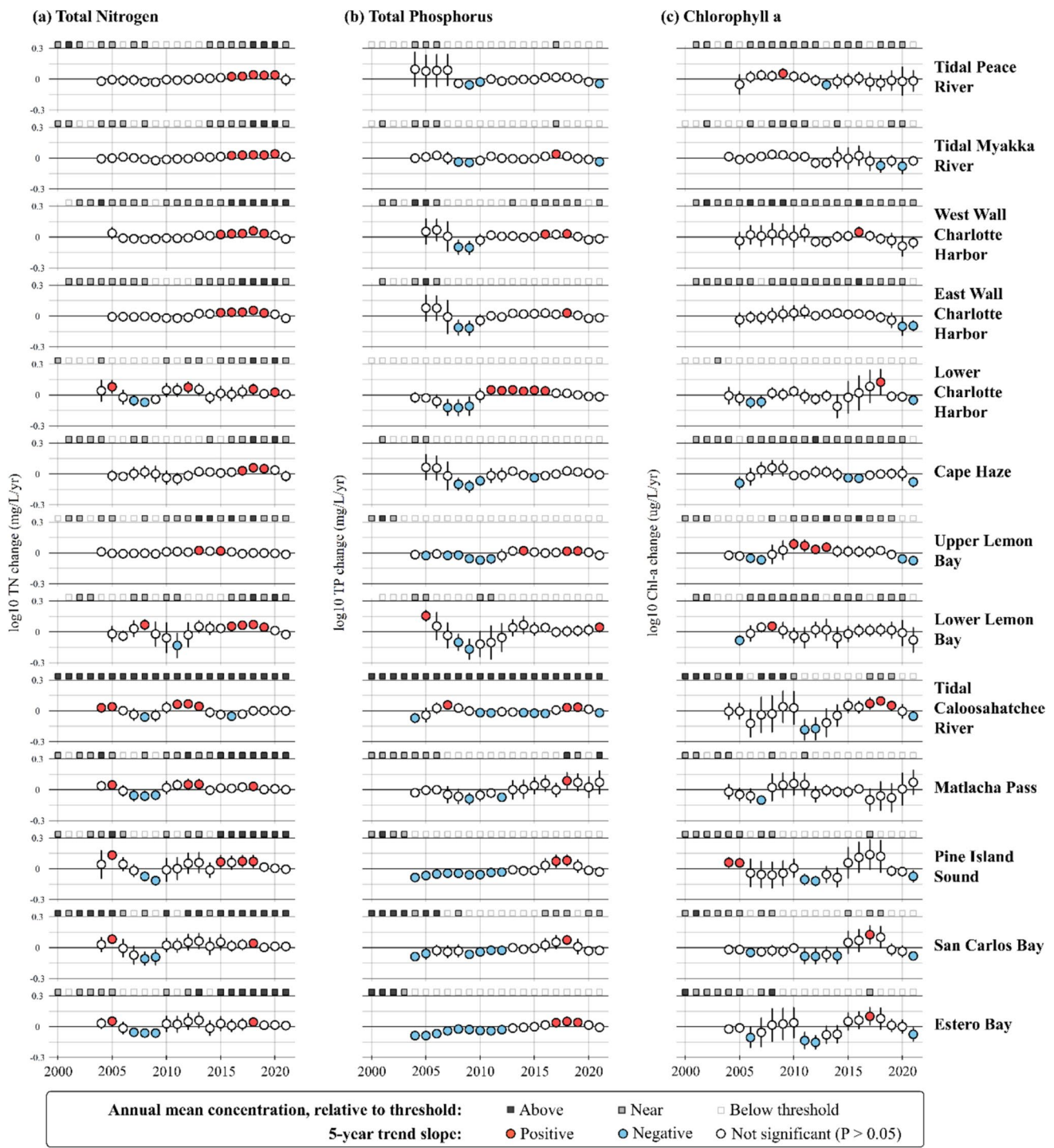


**Fig. 5** Estimated trend slopes over 5-year, right-justified sliding windows, with 95% confidence intervals (CIs), for annual mean concentrations of **a** total nitrogen, **b** total phosphorus, and **c** chlorophyll-a across the 13 CCHMN strata. Within each plot, circles indicate 5-year periods with significant upward trends (red), significant downward trends (blue), and no significant trends (white) ( $\alpha=0.05$ ). Slope val-

ues are assigned to the terminal year of each 5-year window. Above each plot, squares classify annual mean concentrations from the GAM fits relative to stratum-specific thresholds: black squares indicate the 95% confidence interval (CI) of the mean is wholly above the threshold, gray squares indicate the CI overlaps the threshold, and white squares indicate the CI is wholly below the threshold

**Fig. 6** Summary of 2017–2021 annual mean concentration trends for TN, TKN, TP, and chlorophyll-a across all strata, relative to segment-specific thresholds (see Table 2). Symbols indicate trend directions: upward trend (up-arrow), downward trend (down-arrow), or no significant trend (circle). Colors indicate 2021 mean concentrations relative to thresholds: above threshold (red), near threshold (pink), or below threshold (white). Hot spots are defined as strata where the 2021 mean was above the threshold, with an upward trend (red up-arrows; none present) or no significant trend (red circles) between 2017 and 2021

	TN	TKN	TP	Chl-a	
					<b>Tidal Peace River</b>
					<b>Tidal Myakka River</b>
					<b>West Wall Charlotte Harbor</b>
					<b>East Wall Charlotte Harbor</b>
					<b>Lower Charlotte Harbor</b>
					<b>Cape Haze</b>
					<b>Upper Lemon Bay</b>
					<b>Lower Lemon Bay</b>
					<b>Tidal Caloosahatchee River</b>
					<b>Matlacha Pass</b>
					<b>Pine Island Sound</b>
					<b>San Carlos Bay</b>
					<b>Estero Bay</b>

**Symbol Legend:  
Trend Directions**

- ▲ Up ( $P < 0.05$ )
- None ( $P > 0.05$ )
- ▼ Down ( $P < 0.05$ )

**Color Legend:  
2021 Mean Concentration Relative to Threshold**

- Above threshold (Lower CI bound  $>$  threshold)
- Near threshold (CI includes threshold)
- Below threshold (Upper CI bound  $<$  threshold)

concentrations at Lower Lemon Bay exhibited an upward trend and a downward trend during the 5-year windows terminating in 2008 and 2011, respectively, and trended upward during the 5-year windows terminating in 2016 through 2019, reaching a mean concentration of 0.6 mg/L in 2021. At Upper Lemon Bay, annual mean TN concentrations trended upward during the 5-year windows terminating in 2013 and 2015 and otherwise exhibited no trends; the mean concentration in 2021 was 0.5 mg/L.

The Tidal Caloosahatchee River exhibited changes in the 5-year trend direction throughout the study period, with annual mean TN concentrations varying between 0.7 mg/L and 1.5 mg/L during 2000–2014 and stabilizing near 1.0 mg/L during 2014–2021. Annual mean TN concentrations trended upward between 2000 and 2005; downward between 2004 and 2008; upward between 2007 and 2013; and downward between 2012 and 2016 (Figs. 4a and 5a). Lower Charlotte Harbor and other strata to its south

(Matlacha Pass, Pine Island Sound, San Carlos Bay, and Estero Bay) also exhibited shifts in trend direction, with annual mean TN concentrations varying between 0.2 mg/L and 0.9 mg/L during 2000–2014 and stabilizing between 0.7 and 0.9 mg/L during 2014–2021.

Across all strata, annual mean TN concentrations have remained near or above the respective thresholds since 2016 or earlier, and at the Tidal Caloosahatchee River, annual mean TN concentrations exceeded the selected threshold every year (Fig. 5a). From a regulatory perspective, the Tidal Caloosahatchee River stratum comprises three estuarine segments with three separate TMDL target concentrations: the lower segment (0.45 mg/L), middle segment (0.53 mg/L), and upper segment (0.72 mg/L) (FDEP, 2022). We adopted the TMDL target concentration of the lower segment as the threshold (Table 2). Adoption of the highest TMDL target concentration (upper segment, 0.72 mg/L) as the threshold for the Tidal Caloosahatchee stratum would yield similar results, with annual mean TN concentrations exceeding the threshold each year except 2007 and 2008 (“near threshold”).

Nitrogen hot spots (2017–2021) include six of the 13 strata: West Wall, Tidal Caloosahatchee River, Matlacha Pass, Pine Island Sound, San Carlos Bay, and Estero Bay (Fig. 6). In absolute terms, estimated mean TN concentrations in 2021 were greatest at the Tidal Myakka River (1.1 mg/L), Tidal Peace River (1.0 mg/L), and Tidal Caloosahatchee River (1.0 mg/L).

Except for Matlacha Pass, annual mean TN concentrations at each stratum were dominated by organic N forms; annual mean TKN concentrations were near the respective TN concentrations (typically between 0.5 and 1.5 mg/L) with low NH<sub>x</sub>-N concentrations (typically <0.05 mg/L). Notably, the Tidal Caloosahatchee River stratum exhibited annual mean NO<sub>x</sub>-N concentrations that exceeded concentrations at most other strata by approximately one order of magnitude.

## Phosphorus

Across most strata, annual mean TP concentrations in the upper 1 m of the water column remained near or below the respective thresholds since 2007 or earlier (Fig. 5b), with notable exceptions at the Tidal Caloosahatchee River and Matlacha Pass (details below). Recent trends in annual mean TP concentrations varied across strata. Strata with TP concentrations near or below the respective thresholds in 2021 typically exhibited no significant trends during the 2017–2021 window, except for the Tidal Peace and Tidal Myakka Rivers (downward trends) and Lower Lemon Bay (upward trend). Several strata, including the tidal river segments, Lower Charlotte Harbor, and San Carlos Bay, exhibited elevated TP concentrations during one or more months

following Hurricane Irma (September 2017), which appears to have influenced some trend results (upward trends leading up to 2017 or 2018; and/or subsequent downward trends).

At the Tidal Caloosahatchee River, annual mean TP concentrations exceeded the threshold during each year of the study period (2000–2021). This stratum exhibited several downward 5-year trends between the beginning of the record and 2016, upward trends during the 2014–2018 and 2015–2019 windows, and a downward trend during the 2017–2021 window (Figs. 4b and 5b). Matlacha Pass exhibited an upward TP trend during the 2014–2018 window, and annual mean TP concentrations exceeded the threshold in 2018 and 2021 (Fig. 5b). Annual mean TP concentrations at San Carlos Bay were near the threshold in 2016, 2017, 2018, 2020, and 2021, with an upward trend during the 2014–2018 window.

Across most strata, PO<sub>4</sub>-P was the dominant component of annual mean TP concentrations. However, the monthly averaged data suggest that PO<sub>4</sub>-P:TP ratios were relatively low at Lower Lemon Bay, Estero Bay, San Carlos Bay, and Pine Island Sound—the four strata with the lowest mean TP concentrations in 2021 (0.054 mg/L, 0.041 mg/L, 0.041 mg/L, and 0.028 mg/L, respectively). Matlacha Pass was identified as a phosphorus hot spot during 2017–2021, and TP concentrations at the Tidal Caloosahatchee River were elevated during this period with a decreasing trend (Fig. 6). In absolute terms, mean TP concentrations in 2021 were greatest at the Tidal Peace River (0.277 mg/L), Tidal Myakka River (0.212 mg/L), and West Wall (0.178 mg/L).

## Chlorophyll-a

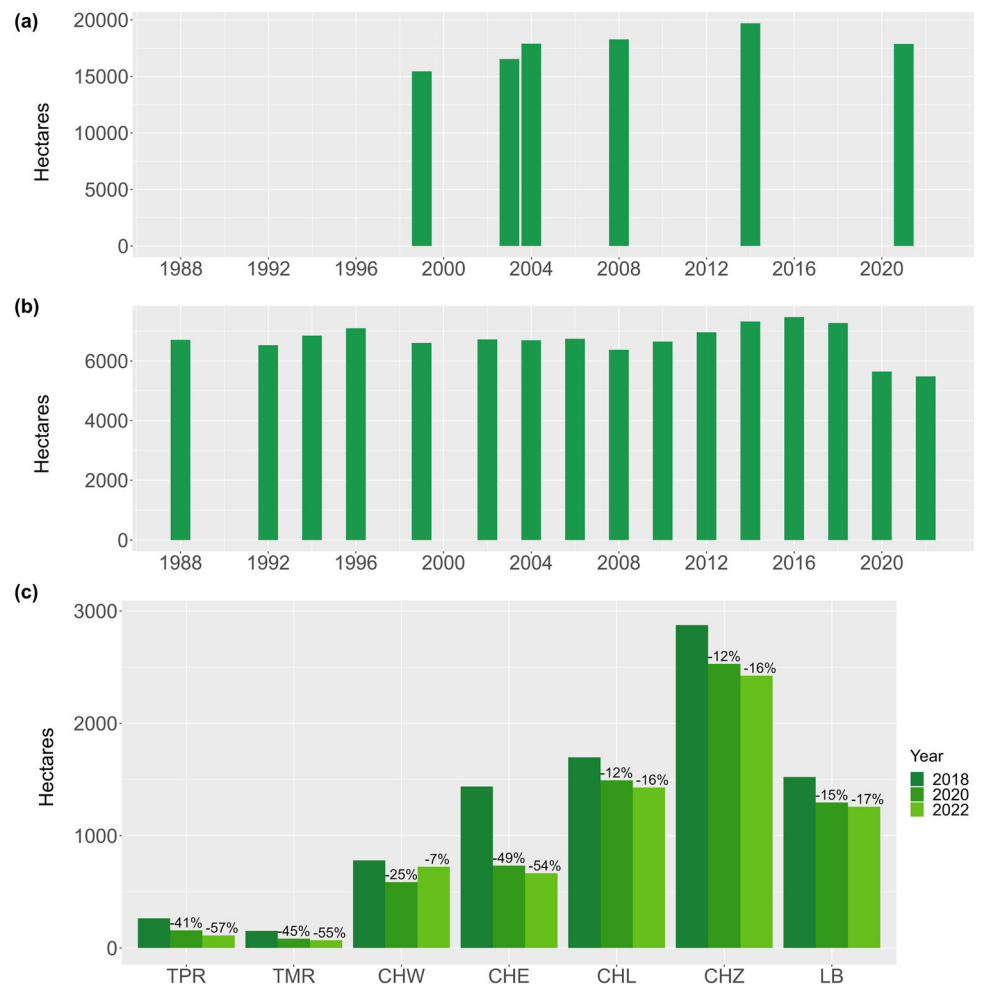
Across all strata, annual mean concentrations of chlorophyll-a exhibited downward trends or no trends during the 2017–2021 window (Fig. 5c), and annual mean concentrations have remained near or below the corresponding thresholds since 2017 or earlier. Further, since 2018, slope estimates have decreased or remained stable across all strata, except for Matlacha Pass, where slope estimates increased substantially between 2019 and 2021 (Fig. 5c). Nonetheless, the 2021 mean concentration at Matlacha Pass (3.2 ug/L) was well below the corresponding threshold (6.1 ug/L).

No chlorophyll-a hot spots were identified for the 2017–2021 period (Fig. 6). In absolute terms, mean chlorophyll-a concentrations in 2021 were greatest at the Tidal Peace River (7.2 ug/L), Tidal Myakka River (5.4 ug/L), and West Wall (4.6 ug/L).

## Seagrass and Macroalgae

Between 1999 and 2014, seagrass coverage generally increased across the southern strata (Fig. 7a) and subsequently declined within most of these strata between 2014

**Fig. 7** Seagrass coverage over time. **a** Aggregate seagrass coverage across the southern strata: Tidal Caloosahatchee River, Matlacha Pass, Pine Island Sound, San Carlos Bay, and Estero Bay. **b** Aggregate seagrass coverage across the Tidal Peace River, Tidal Myakka River, and Charlotte Harbor proper. **c** Changes in seagrass coverage between 2018 and 2022 at Tidal Peace River (TPR), Tidal Myakka River (TMR), West Wall (CHW), East Wall (CHE), Lower Charlotte Harbor (CHL), Cape Haze (CHZ), and Upper and Lower Lemon Bay (LB). Percentages represent losses relative to 2018



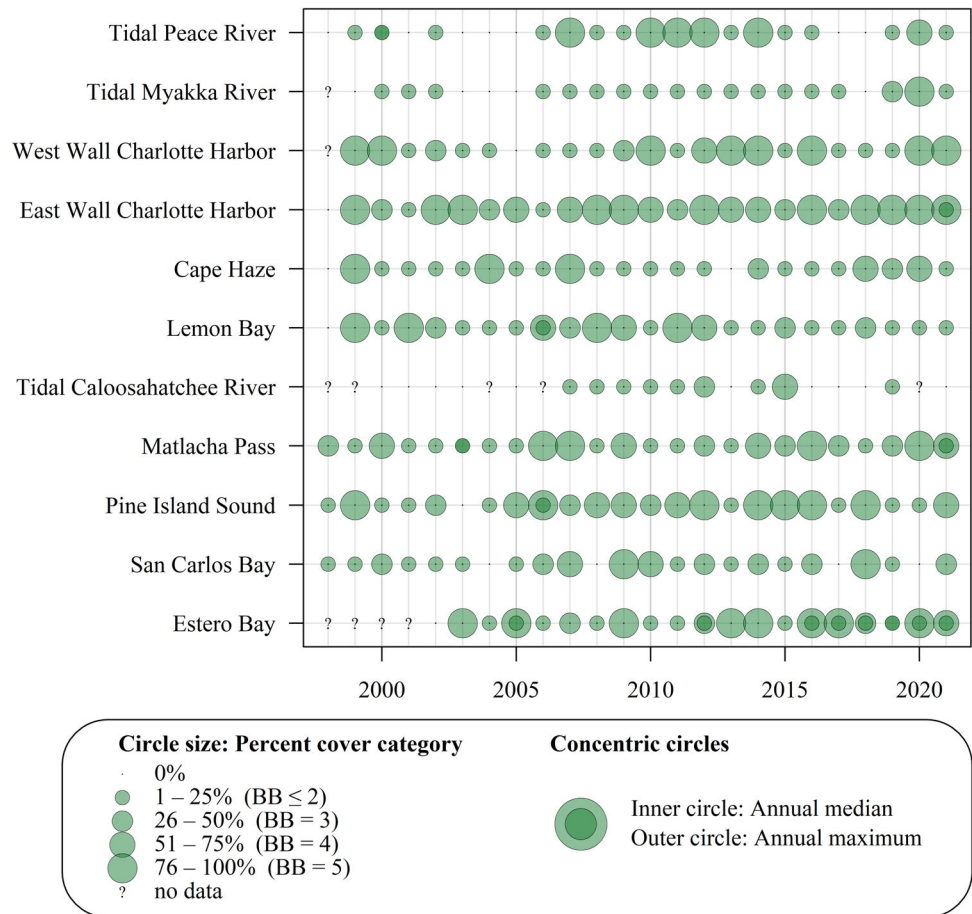
and 2021, including the Tidal Caloosahatchee River (loss of 135 ha, or 70%); Matlacha Pass (loss of 1483 ha, or 44%); San Carlos Bay (loss of 431 ha, or 15%); and Estero Bay (loss of 340 ha, or 23%). At Pine Island Sound, however, seagrass coverage increased by 5% (556 acres) between 2014 and 2021, to 12,335 ha. In 2021, the area of seagrass coverage within Pine Island Sound accounted for 80% of the total seagrass area throughout the southern strata—an increase over previous survey years, during which Pine Island Sound accounted for between 68% (in 1999) and 76% (in 2014).

Between 2018 and 2022, seagrass coverage across the Tidal Peace River, Tidal Myakka River, and Charlotte Harbor proper (i.e., East Wall, West Wall, Lower Charlotte Harbor, and Cape Haze) declined by 25% to the lowest level observed since mapping began in 1988 (Fig. 7b). Losses were observed within each of these strata, with the greatest areal losses occurring along the East Wall and Cape Haze between 2018 and 2020 (Fig. 7c). Between 2020 and 2022, coverage further decreased throughout Charlotte Harbor proper, with the exception of the West Wall.

The distributions of macroalgae transect data collected during the growing season (July–December) each year

between 1998 and 2021 indicated that annual median percent-coverage values have largely remained constant across most strata (zero coverage). One notable exception was Estero Bay, where the medians were consistently greater (in the 1–25% category) during each year between 2016 and 2021 (Fig. 8). Compared to the annual medians, the annual maximum percentage-coverage values have shown greater variability within each stratum. Following Hurricane Irma, maxima increased between 2017 and 2018 at the East Wall, Cape Haze, Lemon Bay, Pine Island Sound, and San Carlos Bay. Subsequently, comparing maxima in 2017 to 2019–2021, the values increased across most strata, often substantially (e.g., Tidal Peace, Tidal Myakka, East Wall, West Wall, Cape Haze, Matlacha Pass). One-sided Mann–Whitney tests indicated that macroalgal coverage significantly increased between the pre- and post-Irma periods (2014–2017 to 2018–2021) at the East Wall ( $W = 44,009$ ,  $P < 0.001$ ), Cape Haze ( $W = 36,357$ ,  $P = 0.011$ ), and Estero Bay ( $W = 31,824$ ,  $P = 0.002$ ). No significant decreases in coverage ( $P > 0.05$ ) were observed between the and pre- and post-Irma periods (see Table S1 for full statistical results).

**Fig. 8** Annual drift macroalgae coverage along transects within each stratum, 1998–2021. Circle sizes correspond to percentage cover categories based on aggregated Braun-Blanquet (BB) scores. Concentric circles indicate the annual median (inner circle) and maximum (outer circle), respectively



### Discussion

This study documents ecological change in the Greater Charlotte Harbor estuaries between 2000 and 2021 with multiple lines of evidence, considering causes (nutrient enrichment), direct effects (phytoplankton and macroalgal production), and indirect effects (seagrass loss) of eutrophication (Clausen et al., 2009). While not directly establishing causation, the results support the hypothesis that nitrogen enrichment during the 2010s contributed to a shift toward macroalgal production and diminished the system’s resilience to acute disturbance, making it more susceptible to the ecological changes observed following Hurricane Irma, consistent with earlier studies (e.g., Milbrandt et al., 2019). These findings underscore the importance of monitoring macroalgal proliferation as an indicator of eutrophication, particularly in systems where the ecological impacts of nutrient enrichment are not fully captured in chlorophyll-a data (CHNEP, 2025). Finally, our findings suggest that addressing the system’s vulnerability to ecological degradation will require adaptive management strategies including traditional nutrient load reductions and complementary interventions.

The Greater Charlotte Harbor estuary is a vast system that comprises several ecologically distinct areas receiving

freshwater flows and nutrient loads from three major rivers and connected through complex hydrodynamics. As such, improvements in water quality, mitigation of harmful algal blooms, and restoration of seagrass and ecological functions throughout the Greater Charlotte Harbor system will require a whole-system approach. Important considerations include (1) current and projected population growth, land use changes, and associated shifts in nutrient loading regimes throughout the watershed, including Lake Okeechobee (Fig. 1a); (2) nutrient assimilative capacity and legacy nutrient accumulation within Greater Charlotte Harbor and its rivers; and (3) restoration goals for the St. Lucie River estuary (southeast Florida) and the Florida Everglades as fellow recipients of Lake Okeechobee discharges (Garcia et al., 2020).

The trend analysis indicated that elevated annual mean TN concentrations in the upper water column were ubiquitous throughout the Greater Charlotte Harbor estuaries between 2010 and 2021 (Figs. 5a and 6). However, the results revealed a contrast between the northern and southern strata. Strata north of Lower Charlotte Harbor generally exhibited relatively stable annual mean concentrations during the first half of the study period, followed by upward trends beginning ca. 2012, whereas the southern strata

exhibited notable variability (i.e., shifts in trend directions) through ca. 2014, followed by a more stable regime (Figs. 4a and S3). Across these southern strata, annual mean TN concentrations converged near 1 mg/L, despite variability in annual TN loads at the S-79 structure during the same period (Tomasko et al., 2024). Interestingly, annual mean TN concentrations at the Tidal Caloosahatchee River converged to values on the *lower* end of the range observed during its earlier variable period (pre-2014), while annual means at the other southern strata converged to values on the *higher* ends of their respective variable-period ranges (e.g., see the plots for Tidal Caloosahatchee River and San Carlos Bay in Fig. 4a). Further research will be needed to better understand spatial differences between northern and southern segments regarding assimilation of nitrogen loads from the watershed, particularly considering active management of Lake Okeechobee releases and Caloosahatchee basin runoff at the S-79 and S-77 flow control structures (Montefiore et al., 2024).

The monthly averaged nitrogen concentration data suggested high TKN:TN ratios throughout the system. Paired with low and often undetected concentrations of inorganic fractions, these results are consistent with nitrogen-limited primary production and rapid biological assimilation of inorganic nitrogen, as reported by earlier studies (Bronk et al., 2014; McPherson et al., 1996; Montgomery et al., 1991; Morrison et al., 1998; Phlips et al., 2023). For context, high TKN:TN ratios are consistent with nitrogen concentrations in riverine discharges. For instance, Rumbold and Doering (2020) reported that between 2009 and 2018, the median TKN concentration in Caloosahatchee River discharges (at the S-79 flow control structure) varied between 1.2 and 1.5 mg/L depending on the magnitude and source of the discharges (basin runoff or Lake Okeechobee), and the organic fraction dominated TKN, with TKN:TN ratios near 0.90 (and low NH<sub>x</sub>-N concentrations). Historically, nitrogen limitation in southwest Florida estuaries has been attributed to abundant dissolved phosphorus originating from rich inland phosphorite deposits and transport associated with mining activity (Fraser & Wilcox, 1981; McPherson et al., 1996; Morrison et al., 1998). Annual mean TP concentrations in the upper water column have remained below the specified thresholds for a decade or more at most strata (Figs. 5b and 6). The Tidal Caloosahatchee River, which conveys managed discharges from the eutrophic Lake Okeechobee, is an important exception.

Across most CCHMN strata, annual mean chlorophyll-*a* concentrations in the upper water column were low relative to their respective thresholds and exhibited downward trends during the 2010 decade (Fig. 5c). Concentrations were highest at the Tidal Peace River, Tidal Myakka River, and West Wall, but none of the strata qualified as a chlorophyll-*a* hot spot during 2017–2021, based on our definition of the term

(Fig. 6). Hydrodynamic modeling by Dye et al. (2020) indicated that Peace River discharges may entrain to the West Wall during the wet season and to both the East Wall and West Wall during the dry season. In contrast, Caloosahatchee River discharges tend to entrain through Matlacha Pass to the East Wall, but not the West Wall, during the wet season. These simulation results suggest that chlorophyll-*a* in the West Wall water column may tend to originate from nutrient loads and/or algal biomass from the Peace and Myakka Rivers, rather than the Caloosahatchee River.

The annual macroalgae transect data exhibited little variability in median coverage throughout the study period, although the annual maxima were more variable (Fig. 8). From 2014–2017 to 2018–2021, increases in macroalgal coverage were statistically significant at the East Wall, Cape Haze, and Estero Bay (Table S1). Although the statistical tests do not directly link these changes to Hurricane Irma or nutrient loading (or any particular cause or event), they clarify which of the changes visualized in Fig. 8 represent statistically significant increases following 2017. Paired with the water quality trend results (low chlorophyll-*a* concentrations and increasing nitrogen concentrations), the macroalgal results suggest that nutrient enrichment has translated into macroalgal production rather than excess phytoplankton production at some strata, although the lack of detectable changes in macroalgae abundance at many strata leaves open questions about the fate of nitrogen inputs. Nonetheless, observed increases in macroalgal abundance are consistent with earlier studies reporting that watershed nitrogen loads fuel macroalgal proliferation in Charlotte Harbor (Lapointe & Bedford, 2007; Milbrandt et al., 2019) as well as studies of other coastal systems in Florida demonstrating that phytoplankton and nutrients in the water column are incomplete indicators of eutrophication (e.g., Lapointe et al., 1994; Scolaro et al., 2023; Tomasko, 2023). Moreover, our findings align with the general tendency of shallow coastal systems to shift biomass production toward macroalgae, rather than phytoplankton, under nutrient enrichment (Burkholder et al., 2007), as demonstrated globally (e.g., Raffaelli et al., 1998; Teichberg et al., 2010). Accordingly, we echo others' calls for increased monitoring of macroalgal abundance based on recognition of macroalgal proliferation as a key symptom of eutrophication along Florida's coasts (e.g., Garcia et al., 2020; Scolaro et al., 2023; Tomasko et al., 2020).

Contemporaneous with these increases in the abundance of benthic macroalgae (Fig. 8; Table S1; Garcia et al., 2020), Charlotte Harbor proper and the Tidal Peace and Myakka Rivers collectively experienced the largest loss of seagrass coverage since mapping efforts began in 1988 (Fig. 7). The East Wall lost more than half of its seagrass coverage, representing the largest areal loss among the northern strata (Fig. 7c). To the south, Matlacha Pass, which is particularly vulnerable to long residence times and associated water

quality issues due to its unique morphology and hydrodynamics (Hewageegana et al., 2023), exhibited the largest areal loss of seagrass among southern strata between the most recent surveys in 2014 and 2021 (SFWMD, 2015; SFWMD, 2022). Likewise, the Tidal Caloosahatchee River, which exceeded specified thresholds for TN and TP concentrations during each year of the study period (Fig. 5), lost 70% of its seagrass between 2014 and 2021 (SFWMD, 2015; SFWMD 2022). In contrast, seagrass coverage increased by 5% at Pine Island Sound between 2014 and 2021, possibly explained by the lesser influence of freshwater and nutrient inputs from the Caloosahatchee River and by tidal flushing via direct connection to the Gulf of Mexico (Dye et al., 2020; Shi et al., 2023). While this study did not explicitly investigate causal relationships among nutrient enrichment, algal production, and seagrass losses, the curated dataset and results presented here represent a foundation for further research in this direction.

Two major (and possibly related) disturbances—Hurricane Irma in September 2017 and a prolonged *K. brevis* bloom event between October 2017 and January 2019—likely played a role in macroalgal proliferation and seagrass losses observed throughout the system. However, these changes occurred within the context of elevated nitrogen concentrations that had already begun to trend upward prior to the onset of these disturbances (Fig. 5a). Therefore, we suspect that nutrient enrichment during the 2010s—in particular, increasing nitrogen trends beginning ca. 2012—may have made the system more vulnerable to the profound ecological changes that followed Hurricane Irma.

In addition, we speculate that large releases from Lake Okeechobee during the 90 days following passage of Hurricane Irma in 2017 may partially explain observed spatial differences in the timing of subsequent macroalgal proliferation: Whereas increased abundances were observed at southern transects (San Carlos Bay and Pine Island Sound) and East Wall transects in 2018, similar increases were not observed until subsequent years at other northern transects (West Wall, Tidal Myakka, and Tidal Peace). The increased abundance at the East Wall in 2018 may be consistent with this hypothesis, because Caloosahatchee River discharges reach the East Wall via Matlacha Pass relatively rapidly during periods of high discharge (Dye et al., 2020). Fish kills associated with the 2017–2019 *K. brevis* bloom event (Griffin et al., 2023; McCabe et al., 2021) may have ultimately altered nutrient cycling and shallow benthic communities sufficiently to further stimulate later macroalgal production throughout the system.

### Comments on the Trend Analysis Methodology

The GAM-based framework can effectively capture non-linear inter-annual dynamics and intra-annual (seasonal)

cycles while accommodating data gaps and accounting for uncertainty (Beck et al., 2022). Although our analysis focused on trends in annual means, one could likewise apply the methodology to identify trends in other metrics or to restrict the analysis to a particular season—for instance, trends in wet-season chlorophyll-a maxima or dissolved oxygen minima. Combined, the framework's flexibility and treatment of uncertainty provide multiple advantages for detecting water quality trends compared to more conventionally applied methods.

We interpreted the trend results for nitrogen, phosphorus, and chlorophyll-a in the context of segment-specific thresholds to identify high-priority hot spots, where a hot spot was defined as a stratum whose most recent annual mean concentration exceeded the threshold and which most recently exhibited no trend or an upward trend. However, different types of thresholds may be applied to serve different objectives—for instance, thresholds based on known ecological limits or on restoration or management goals. Further, the integration of trend results with absolute thresholds produces a matrix of combinations that can be grouped into multiple management-relevant categories. For instance, a “sensitive/emerging concern” category would describe cases with values near the threshold (with no trend or an upward trend) and cases with values below the threshold (and an upward trend). Such a multi-level prioritization scheme would provide additional management value beyond the common binary regulatory paradigm (impaired or not impaired). Inclusion of ecological indicators (e.g., seagrass and macroalgae) provides further context for interpretation of water quality trends.

Finally, the approach demonstrated in this study provides a model for robustly tracking and understanding water quality and eutrophication over time in other estuaries throughout Florida and beyond, with a spatially stratified sampling design for long-term water quality monitoring, GAM-based water quality trend analysis and hot spot analysis, and regular monitoring of seagrass and macroalgae. Long-term monitoring of other nutrient compartments (e.g., lower water column and benthic sediments) and more sensitive detection of inorganic nutrients (e.g.,  $\text{NH}_x\text{-N}$ ) in the water column would enable a more comprehensive understanding of nutrient pathways and ecological health. The results of trend and hot spot analyses provide a basis for placing management interventions and disturbance events in a historical context, tracing estuarine eutrophication to upstream point and non-point pollutant sources in the watershed, and targeting future management and restoration interventions.

**Supplementary Information** The online version contains supplementary material available at <https://doi.org/10.1007/s12237-025-01488-2>.

**Acknowledgements** The authors thank Melynda Brown and Arielle Taylor-Manges at FDEP for their assistance in assembling and interpreting the macroalgae transect data.

**Authors' Contributions** All authors contributed to the study conception and design, active execution of the study, and interpretation of data and results. The first draft of the manuscript was written by MM and all authors commented on previous versions of the manuscript. All authors read and approved the final manuscript.

**Funding** Florida Department of Environmental Protection (Agreement Number LPR0017) and the Coastal & Heartland National Estuary Partnership (U.S. Environmental Protection Agency Agreement Number CE-00D90019-2).

**Data Availability** The curated water quality dataset is available at <http://doi.org/https://doi.org/10.17605/OSF.IO/WDZ45> (Medina, 2024).

## Declarations

**Competing Interest** The authors declare no competing interests.

## References

- Anderson, D. M., Fensin, E., Gobler, C. J., Hoeglund, A. E., Hubbard, K. A., Kulis, D. M., Landsberg, J. H., Lefebvre, K. A., Provoost, P., Richlen, M. L., Smith, J. L., Solow, A. R., & Trainer, V. L. (2021). Marine harmful algal blooms (HABs) in the United States: History, current status and future trends. *Harmful Algae*, 102, 101975. <https://doi.org/10.1016/j.hal.2021.101975>
- Beck, M. W., de Valpine, P., Murphy, R., Wren, I., Chelsky, A., Foley, M., & Senn, D. B. (2022). Multi-scale trend analysis of water quality using error propagation of generalized additive models. *Science of the Total Environment*, 802, 149927. <https://doi.org/10.1016/j.scitotenv.2021.149927>
- Beck, M. W., Robison, D. E., Raulerson, G. E., Burke, M. C., Saarinen, J., Sciarrino, C., Sherwood, E. T., & Tomasko, D. A. (2023). Addressing climate change and development pressures in an urban estuary through habitat restoration planning. *Frontiers in Ecology and Evolution*, 11, 1–15. <https://doi.org/10.3389/fevo.2023.1070266>
- Brand, L. E., & Compton, A. (2007). Long-term increase in *Karenia brevis* abundance along the Southwest Florida coast. *Harmful Algae*, 6(2), 232–252. <https://doi.org/10.1016/j.hal.2006.08.005>
- Bronk, D. A., Killberg-Thoreson, L., Sipler, R. E., Mulholland, M. R., Roberts, Q. N., Bernhardt, P. W., Garrett, M., O'Neill, J. M., & Heil, C. A. (2014). Nitrogen uptake and regeneration (ammonium regeneration, nitrification and photoproduction) in waters of the West Florida shelf prone to blooms of *Karenia brevis*. *Harmful Algae*, 38, 50–62. <https://doi.org/10.1016/j.hal.2014.04.007>
- Burkholder, J. M., Tomasko, D. A., & Touchette, B. W. (2007). Seagrasses and eutrophication. *Journal of Experimental Marine Biology and Ecology*, 350, 46–72. <https://doi.org/10.1016/j.jembe.2007.06.024>
- Charlotte Harbor National Estuary Program [CHNEP]. (2004). *Coastal Charlotte Harbor Monitoring Network Description and Standard Operating Procedures*. CHNEP Technical Report 02–03. Charlotte Harbor National Estuary Program, Punta Gorda, FL. <https://chnep.wateratlas.usf.edu/>. Accessed Jan 2024.
- Claussen, U., Zevenboom, W., Brockmann, U., Topcu, D., & Bot, P. (2009). Assessment of the eutrophication status of transitional, coastal and marine waters within OSPAR. *Hydrobiologia*, 629, 49–58. <https://doi.org/10.1007/s10750-009-9763-3>
- Cloern, J. E. (2001). Our evolving conceptual model of the coastal eutrophication problem. *Marine Ecology Progress Series*, 210, 223–253. <https://doi.org/10.3354/meps210223>
- Coastal & Heartland National Estuary Partnership [CHNEP]. (2019). *Coastal Charlotte Harbor Monitoring Network: Standard Operating Procedures, 2019 Updates*. <https://chnep.wateratlas.usf.edu/>. Accessed Jan 2024.
- Coastal & Heartland National Estuary Partnership [CHNEP]. (2023). *Coastal Charlotte Harbor Monitoring Network Standard Operating Procedures and Quality Assurance Plan 2023 Updates*. Charlotte Harbor National Estuary Program Technical Report 15–4. <https://chnep.wateratlas.usf.edu/>. Accessed Jan 2024.
- Coastal & Heartland National Estuary Partnership [CHNEP]. (2025). *Protecting our water, wildlife, and future: 2025 Comprehensive Conservation and Management Plan for the CHNEP Area in Central and Southwest Florida*. Update 2025, p 219. <http://www.chnep.org>. Accessed Jan 2025.
- Corbett, C. A., & Hale, J. A. (2006). Development of water quality targets for Charlotte Harbor, Florida using seagrass light requirements. *Florida Scientist*, 69(2), 36–50.
- Croghan, C. W., & Egeghy, P. P. (2003). *Methods of dealing with values below the limit of detection using SAS*. North Carolina State University, Institute for Advanced Analytics, Raleigh, NC. <http://analytics.ncsu.edu/sesug/2003/SD08-Croghan.pdf>. Accessed Sep 2024.
- Duffrey, R., Leary R. E., & Ott, J. (2007). *Water quality status & trends for 1998–2005: Final Report*. Charlotte Harbor Aquatic Preserves Technical Report #2. <https://chnep.wateratlas.usf.edu/upload/documents/CHEVWQMN2007.pdf>. Accessed Jan 2024.
- Dunic, J. C., Brown, C. J., Connolly, R. M., Turschwell, M. P., & Côté, I. M. (2021). Long-term declines and recovery of meadow area across the world's seagrass bioregions. *Global Change Biology*, 27, 4096–4109. <https://doi.org/10.1111/gcb.15684>
- Dye, B., Jose, F., & Allahdadi, M. N. (2020). Circulation dynamics and seasonal variability for the Charlotte Harbor estuary, Southwest Florida coast. *Journal of Coastal Research*, 36(2), 276–288. <https://doi.org/10.2112/JCOASTRES-D-19-00071.1>
- Florida Department of Environmental Protection [FDEP]. (2019). Standard procedures for seagrass monitoring for the Charlotte Harbor Aquatic Preserves' seagrass transect monitoring program. Punta Gorda, Florida.
- Florida Department of Environmental Protection [FDEP]. (2022). Biennial Assessment 2020–2022 (All Groups). <https://floridadep.gov/dear/watershed-assessment-section/content/assessment-lists>. Accessed Jan 2024.
- Florida Department of Environmental Protection [FDEP] and Charlotte Harbor Aquatic Preserves [CHAP]. (2024). Seagrass monitoring data .
- Fraser, T. H., & Wilcox, W. H. (1981). Enrichment of a subtropical estuary with nitrogen, phosphorus and silica. In B. J. Neilson, & L. E. Cronin (Eds.), *Estuaries and nutrients*. Clifton, New Jersey: Humana Press.
- Garcia, L., Anastasiou, C., & Tomasko, D. (2020). *Charlotte Harbor Surface Water Improvement and Management (SWIM) Plan*. Southwest Florida Water Management District, Brooksville, Florida. <https://chnep.wateratlas.usf.edu/upload/documents/Charlotte-Harbor-SWIM-Plan-Nov2020-FINAL.pdf>. Accessed Dec 2023.
- Griffin, L. P., Friess, C., Bakenhaster, M. D., Bassos-Hull, K., Burnsed, S. W., Brownscombe, J. W., Cooke, S. J., Ellis, R. D., Gardiner, J. M., Locascio, J., Lowerre-Barbieri, S., Poulakis, G. R., Wiley, T. R., Wilkinson, K. A., Wilson, J. K., Wooley, A. K., Adams, A. J., & Danylchuk, A. J. (2023). Assessing the potential for red tide (*Karenia brevis*) algal bloom impacts on Atlantic tarpon (*Megalops atlanticus*) along the southwestern coast of Florida. *Environmental Biology of Fishes*, 106, 255–273. <https://doi.org/10.1007/s10641-022-01324-7>

- Grolemund, G., & Wickham, H. (2011). Dates and times made easy with lubridate. *Journal of Statistical Software*, 40(3), 1–25. <https://www.jstatsoft.org/v40/i03/>.
- Hastie, T., & Tibshirani, R. (1986). Generalized additive models. *Statistical Science*, 1(3), 297–310. <http://www.jstor.org/stable/2245459>
- Heil, C. A., Dixon, L. K., Hall, W., Garrett, M., Lenes, J. M., O’Neil, J. M., Walsh, B. M., Bronk, D. A., Killberg-Thoreson, L., Hitchcock, G. L., Meyer, K. A., Mulholland, M. R., Procise, L., Kirkpatrick, G. J., Walsh, J. J., & Weisberg, R. W. (2014). Blooms of *Karenia brevis* (Davis) G. Hansen & Ø. Moestrup on the West Florida Shelf: Nutrient sources and potential management strategies based on a multiyear regional study. *Harmful Algae*, 38, 127–140. <https://doi.org/10.1016/j.hal.2014.07.016>
- Hewageegana, V. H., Olabarieta, M., & Gonzalez-Ondina, J. M. (2023). Main physical processes affecting the residence times of a micro-tidal estuary. *Journal of Marine Science and Engineering*, 11(7), 1333. <https://doi.org/10.3390/jmse11071333>
- Hirsch, R. M., Slack, J. R., & Smith, R. A. (1982). Techniques of trend analysis for monthly water quality data. *Water Resources Research*, 18(1), 107–121. <https://doi.org/10.1029/WR018i001p00107>
- Julian, P., II., Thompson, M., & Milbrandt, E. C. (2024). Dark waters: Evaluating seagrass community response to optical water quality and freshwater discharges in a highly managed subtropical estuary. *Regional Studies in Marine Science*, 69, 103302. <https://doi.org/10.1016/j.rsma.2023.103302>
- Kim, T., Sheng, Y. P., & Park, K. (2010). Modeling water quality and hypoxia dynamics in Upper Charlotte Harbor, Florida, U.S.A. during 2000. *Estuarine, Coastal and Shelf Science*, 90(4), 250–263. <https://doi.org/10.1016/j.ecss.2010.09.006>
- Lapointe, B. E., Tomasko, D. A., & Matzie W. R. (1994). Eutrophication and trophic state classification of seagrass communities in the Florida Keys. *Bulletin of Marine Science*, 54, 696–717. <https://api.semanticscholar.org/CorpusID:35139386>
- Lapointe, B. E., & Bedford, B. J. (2007). Drift rhodophyte blooms emerge in Lee County, Florida, USA: Evidence of escalating coastal eutrophication. *Harmful Algae*, 6(30), 421–437. <https://doi.org/10.1016/j.hal.2006.12.005>
- Ma, P., Zhang, L., & Mitsch, W. J. (2020). Investigating sources and transformations of nitrogen using dual stable isotopes for Lake Okeechobee restoration in Florida. *Ecological Engineering*, 155, 105947. <https://doi.org/10.1016/j.ecoleng.2020.105947>
- Malone, T. C., & Newton, A. (2020). The globalization of cultural eutrophication in the coastal ocean: Causes and consequences. *Frontiers in Marine Science*, 7, 670. <https://doi.org/10.3389/fmars.2020.00670>
- McCabe, E. J. B., Wells, R. S., Toms, C. N., Barleycorn, A. A., Wilkinson, K. A., & Palubok, V. I. (2021). Effects of multiple *Karenia brevis* red tide blooms on a common bottlenose dolphin (*Tursiops truncatus*) prey fish assemblage: Patterns of resistance and resilience in Sarasota Bay. *Florida. Frontiers in Marine Science*, 8, 711114. <https://doi.org/10.3389/fmars.2021.711114>
- McPherson, B. F., Miller, R. L., & Stoker, Y. E. (1996). *Physical, chemical, and biological characteristics of the Charlotte Harbor Basin and estuarine system in southwestern Florida—A summary of the 1982–1989 U.S. Geological Survey Charlotte Harbor Assessment and other studies*. Water-Supply Paper 2486. U. S. Geological Survey. [https://fl.water.usgs.gov/PDF\\_files/wsp2486\\_mcpherson.pdf](https://fl.water.usgs.gov/PDF_files/wsp2486_mcpherson.pdf). Accessed Nov 2023.
- Medina, M. (2024). Coastal Charlotte Harbor Monitoring Network (CCHMN) Water Quality Dataset 2000–2021, Version 1.1. <https://doi.org/10.17605/OSF.IO/WDZ45>
- Medina, M., Huffaker, R., Jawitz, J. W., & Muñoz-Carpena, R. (2020). Seasonal dynamics of terrestrially sourced nitrogen influence *Karenia brevis* blooms of Florida’s southern Gulf Coast. *Harmful Algae*, 98, 101900. <https://doi.org/10.1016/j.hal.2020.101900>
- Medina, M., Kaplan, D., Milbrandt, E. C., Tomasko, D., Huffaker, R., & Angelini, C. (2022). Nitrogen-enriched discharges from a highly managed watershed intensify red tide (*Karenia brevis*) blooms in southwest Florida. *Science of the Total Environment*, 827, 154149. <https://doi.org/10.1016/j.scitotenv.2022.154149>
- Milbrandt, E. C., Martignette, A. J., Thompson, M. A., Bartleson, B. D., Phelps, E. J., Badylak, S., & Nelson, N. G. (2021). Geospatial distribution of hypoxia associated with a *Karenia brevis* bloom. *Estuarine, Coastal and Shelf Science*, 259, 107446. <https://doi.org/10.1016/j.ecss.2021.107446>
- Milbrandt, E. C., Reidenbach, L., & Parsons, M. (2019). Determining the sources of macroalgae during beach stranding events from species composition, stable isotope analysis, and laboratory experiments. *Estuaries and Coasts*, 42(3), 719–730. <https://doi.org/10.1007/s12237-018-00489-8>
- Montefiore, L. R., Kaplan, D., Phelps, E. J., Milbrandt, E. C., Arias, M. E., Morrison, E., & Nelson, N. G. (2024). Downstream nutrient concentrations depend on watershed inputs more than reservoir releases in a highly engineered watershed. *Water Resources Research*, 60, e2023WR035590. <https://doi.org/10.1029/2023WR035590>
- Montgomery, R. T., McPherson B. F., & Emmons, E. E. (1991). *Effects of nitrogen and phosphorus additions on phytoplankton productivity and chlorophyll a in a subtropical estuary, Charlotte Harbor, Florida*. U.S. Geological Survey, *Water Resources Investigations Report 91–4077*. Tallahassee, Florida. <https://pubs.usgs.gov/publication/wri914077>. Accessed Nov 2023.
- Morrison, G., Montgomery, R., Squires, A., Starks, R., DeHaven, E., & Ott, J. (1998). Nutrient, chlorophyll and dissolved oxygen concentrations in Charlotte Harbor: Existing conditions and long-term trends. In S.F. Treat (Eds.), *Proceedings of the Charlotte Harbor Public Conference and Technical Symposium*. Charlotte Harbor National Estuary Program Technical Report No. 98–02. <https://polk.wateratlas.usf.edu/upload/documents/MorrisonEtAl-1997-Chl-and-DO-CharHarbSymposiumUpdated.pdf>. Accessed Jan 2024.
- Morrison, E. S., Phelps, E., Badylak, S., Chappel, A. R., Altieri, A. H., Osborne, T. Z., Tomasko, D., Beck, M. W., & Sherwood, E. (2023). The response of Tampa Bay to a legacy mining nutrient release in the year following the event. *Frontiers in Ecology and Evolution*, 11, 1144778. <https://doi.org/10.3389/fevo.2023.1144778>
- National Drought Mitigation Center [NDMC], U.S. Department of Agriculture [USDA], and National Oceanic and Atmospheric Administration [NOAA]. (2024). United States Drought Monitor Data: Time Series. Retrieved from <https://droughtmonitor.unl.edu/DmData/TimeSeries.aspx>. Updated January 2024. Accessed January 2024.
- National Oceanic and Atmospheric Administration [NOAA] Office of Coast Survey. (2015). Nautical Chart 11426: Estero Bay to Lemon Bay including Charlotte Harbor. <https://www.charts.noaa.gov/PDFs/11426.pdf>
- Orth, R. J., Carruthers, T. J. B., Dennison, W. C., Duarte, C. M., Fourqurean, J. W., Heck, K. L., Hughes, A. R., Kendrick, G. A., Judson Kenworthy, W., Olyarnik, S., Short, F. T., Waycott, M., & Williams, S. L. (2006). A global crisis for seagrass ecosystems. *BioScience*, 56(12), 987–996. [https://doi.org/10.1641/0006-3568\(2006\)56\[987:AGCFSE\]2.0.CO;2](https://doi.org/10.1641/0006-3568(2006)56[987:AGCFSE]2.0.CO;2)
- Paerl, H. W. (2009). Controlling eutrophication along the freshwater–marine continuum: Dual nutrient (N and P) reductions are essential. *Estuaries and Coasts*, 32, 593–601. <https://doi.org/10.1007/s12237-009-9158-8>
- Pannard, A., Souchu, P., Chauvin, C., Delabuis, M., Gascuel-Oudou, C., Jeppesen, E., Le Moal, M., Menesguen, A., Pinay, G.,

- Rabalais, N. N., Souchon, Y., & Gross, E. M. (2024). Why are there so many definitions of eutrophication? *Ecological Monographs*, 94(3), e1616. <https://doi.org/10.1002/ecm.1616>
- Phlips, E. J., Badylak, S., Mathews, A. L., Milbrandt, E. C., Montefiore, L. R., Morrison, E. S., Nelson, N., & Stelling, B. (2023). Algal blooms in a river-dominated estuary and nearshore region of Florida, USA: The influence of regulated discharges from water control structures on hydrologic and nutrient conditions. *Hydrobiologia*, 850, 4385–4411. <https://doi.org/10.1007/s10750-022-05135-w>
- Pierce, R. H., Wetzel, D. L., & Estevez, E. D. (2004). Charlotte Harbor initiative: Assessing the ecological health of southwest Florida's Charlotte Harbor estuary. *Ecotoxicology*, 13, 275–284. <https://doi.org/10.1023/B:ECTX.0000023571.55816.2c>
- R Core Team. (2023). *R: A language and environment for statistical computing*. R Foundation for Statistical Computing, Vienna, Austria. <https://www.R-project.org>
- Raffaelli, D. G., Raven, J. A., & Poole, L. J. (1998). Ecological impact of green macroalgal blooms. In A. D. Ansell, R. N. Gibson, & M. Barnes (Eds.), *Oceanography and marine biology: An annual review*. CRC Press. <https://www.taylorfrancis.com/chapters/edit/10.1201/b12646-13/ecological-impact-green-macroalgal-blooms-david-raffaelli-john-raven-lynda-poole>. Accessed Jan 2024.
- Rumbold, D. G., & Doering, P. H. (2020). Water quality and source of freshwater discharge to the Caloosahatchee Estuary, Florida: 2009–2018. *Florida Scientist*, 83(1), 1–20.
- Schiff, K., Trowbridge, P. R., Sherwood, E. T., Tango, P., & Batiuk, R. A. (2016). Regional monitoring programs in the United States: Synthesis of four case studies from Pacific, Atlantic, and Gulf Coasts. *Regional Studies in Marine Science*, 4, A1–A7. <https://doi.org/10.1016/j.risma.2015.11.007>
- Scolaro, S., Beck, M. W., Burke, M. C., Raulerson, G. E., & Sherwood, E. T. (2023). Piney Point, seagrass, and macroalgae: Impact assessment and a case for enhanced macroalgae monitoring. *Florida Scientist*, 86(2), 339–345.
- Sera, F., Armstrong, B., Blangiardo, M., & Gasparrini, A. (2019). An extended mixed-effects framework for meta-analysis. *Statistics in Medicine*, 38(29), 5429–5444. <https://doi.org/10.1002/sim.8362>
- Shi, L., Ortals, C., Valle-Levinson, A., & Olabarrieta, M. (2023). Influence of river discharge on tidal and subtidal flows in a microtidal estuary: Implication on velocity asymmetries. *Advances in Water Resources*, 177, 104446. <https://doi.org/10.1016/j.advwatres.2023.104446>
- South Florida Water Management District [SFWMD]. (2001). West Coast Seagrass Communities (1999). Retrieved from: <https://geo-sfwmd.hub.arcgis.com/datasets/sfwmd::west-coast-seagrass-communities-1999/>. Updated October 2023. Accessed January 2024.
- South Florida Water Management District [SFWMD]. (2004). West Coast Seagrass Communities (2003). Retrieved from: <https://geo-sfwmd.hub.arcgis.com/datasets/sfwmd::west-coast-seagrass-communities-2003/>. Updated October 2023. Accessed January 2024.
- South Florida Water Management District [SFWMD]. (2006). West Coast Seagrass Communities (2004). Retrieved from: <https://geo-sfwmd.hub.arcgis.com/datasets/sfwmd::west-coast-seagrass-communities-2004/>. Updated October 2023. Accessed January 2024.
- South Florida Water Management District [SFWMD]. (2009). West Coast Seagrass Communities (2008). Retrieved from: <https://geo-sfwmd.hub.arcgis.com/datasets/sfwmd::west-coast-seagrass-communities-2008/>. Updated October 2023. Accessed January 2024.
- Southwest Florida Water Management District [SFWMD]. (2010). Proposed minimum flows and levels for the lower peace river and shell creek, final report and Appendix 1. [https://www.sfwmd.state.fl.us/sites/default/files/documents-and-reports/reports/lower\\_peace\\_river\\_report.pdf](https://www.sfwmd.state.fl.us/sites/default/files/documents-and-reports/reports/lower_peace_river_report.pdf)
- South Florida Water Management District [SFWMD]. (2015). West Coast Seagrass Communities (2014). Retrieved from: <https://geo-sfwmd.hub.arcgis.com/datasets/sfwmd::west-coast-seagrass-communities-2014/>. Updated October 2023. Accessed January 2024.
- Southwest Florida Water Management District [SFWMD]. (2019). Seagrass in 2018. Retrieved from <https://data-sfwmd.opendata.arcgis.com/datasets/sfwmd::seagrass-in-2018>. Updated November 2021. Accessed January 2024.
- South Florida Water Management District [SFWMD]. (2022). West Coast Seagrass Communities (2021). Retrieved from: <https://geo-sfwmd.hub.arcgis.com/datasets/sfwmd::west-coast-seagrass-communities-2021/>. Updated October 2023. Accessed January 2024.
- Southwest Florida Water Management District [SFWMD]. (2021). Seagrass in 2020. Retrieved from <https://data-sfwmd.opendata.arcgis.com/datasets/sfwmd::seagrass-in-2020>. Updated November 2021. Accessed January 2024.
- Southwest Florida Water Management District [SFWMD]. (2023). Seagrass in 2022. Retrieved from <https://data-sfwmd.opendata.arcgis.com/datasets/sfwmd::seagrass-in-2022>. Updated February 2023. Accessed January 2024.
- Steinman, A. D., Havens, K. E., Carrick, H. J., & Vanzee, R. (2002). The past, present, and future hydrology and ecology of Lake Okeechobee and its watersheds. In J. W. Porter & K. G. Porter (Eds.), *The Everglades, Florida Bay, and Coral Reefs of the Florida Keys: An Ecosystem Sourcebook*. CRC Press. <https://www.taylorfrancis.com/chapters/mono/10.1201/9781420039412-5/past-present-future-hydrology-ecology-lake-okeechobee-watersheds-james-porter>. Accessed Jan 2024.
- Teichberg, M., Fox, S. E., Olsen, Y. S., Valiela, I., Martinetto, P., Iribarne, O., Muto, E. Y., Petti, M. A. V., Corbisier, T. N., Soto-Jimenez, M., Paez-Osuna, F., Castro, P., Freitas, H., Zitteli, A., Cardinaletti, M., & Tagliapietra, D. (2010). Eutrophication and macroalgal blooms in temperate and tropical coastal waters: Nutrient enrichment experiments with *Ulva* spp. *Global Change Biology*, 16, 2624–2637. <https://doi.org/10.1111/j.1365-2486.2009.02108.x>
- Tomasko, D. (2023). Ecological impacts to Sarasota Bay from Piney Point discharges—Examining the evidence. *Florida Scientist*, 86(2), 301–313.
- Tomasko, D., Alderson, M., Burnes, R., Hecker, J., Iadevaia, N., Leverone, J., Raulerson, G., & Sherwood, E. (2020). The effects of Hurricane Irma on seagrass meadows in previously eutrophic estuaries in Southwest Florida (USA). *Marine Pollution Bulletin*, 156, 111247. <https://doi.org/10.1016/j.marpolbul.2020.111247>
- Tomasko, D., Alderson, M., Burnes, R., Hecker, J., Leverone, J., Raulerson, G., & Sherwood, E. (2018). Widespread recovery of seagrass coverage in southwest Florida (USA): Temporal and spatial trends and management actions responsible for success. *Marine Pollution Bulletin*, 135, 1128–1137. <https://doi.org/10.1016/j.marpolbul.2018.08.049>
- Tomasko, D. A., Anastasiou, C., & Kovach, C. (2006). Dissolved oxygen dynamics in Charlotte Harbor and its contributing watershed, in response to hurricanes Charley, Frances, and Jeanne—Impacts and recovery. *Estuaries and Coasts: J ERF*, 29, 932–938. <https://doi.org/10.1007/BF02798653>
- Tomasko, D. A., Corbett, C. A., Greening, H. S., & Raulerson, G. E. (2005). Spatial and temporal variation in seagrass coverage in southwest Florida: Assessing the relative effects of anthropogenic nutrient load reduction and rainfall in four contiguous estuaries. *Marine Pollution Bulletin*, 50, 797–805. <https://doi.org/10.1016/j.marpolbul.2005.02.010>

- Tomasko, D., Landau, L., Suau, S., Medina, M., & Hecker, J. (2024). An evaluation of the relationships between the duration of red tide (*Karenia brevis*) blooms and watershed nitrogen loads in south-west Florida (USA). *Florida Scientist*, 87(2), 61–72.
- Turner, R. E., Rabalais, N. N., Fry, B., Atilla, N., Milan, C. S., Lee, J. M., & Tomasko, D. A. (2006). Paleo-indicators and water quality change in the Charlotte Harbor estuary (Florida). *Limnology and Oceanography*, 51(1), 518–533. [https://doi.org/10.4319/lo.2006.51.1\\_part\\_2.0518](https://doi.org/10.4319/lo.2006.51.1_part_2.0518)
- Vargo, G. A. (2009). A brief summary of the physiology and ecology of *Karenia brevis* Davis (G. Hansen and Moestrup comb. nov.) red tides on the West Florida Shelf and of hypotheses posed for their initiation, growth, maintenance, and termination. *Harmful Algae*, 8, 573–584. <https://doi.org/10.1016/j.hal.2008.11.002>
- Wickham, H. (2011). The split-apply-combine strategy for data analysis. *Journal of Statistical Software*, 40(1), 1–29. <https://www.jstatsoft.org/v40/i01/>
- Wickham, H., Francois, R., Henry, L., Muller, K., & Vaughan, D. (2023). dplyr: A grammar of data manipulation. R package version 1.1.2. <https://CRAN.R-project.org/package=dplyr>
- Wood, S. N. (2017). *Generalized additive models: An introduction with R* (2nd ed.). Chapman and Hall/CRC. <https://doi.org/10.1201/9781315370279>
- Wood, S. N. (2011). Fast stable restricted maximum likelihood and marginal likelihood estimation of semiparametric generalized linear models. *Journal of the Royal Statistical Society: Series B (Statistical Methodology)*, 73(1), 3–36.

**Publisher's Note** Springer Nature remains neutral with regard to jurisdictional claims in published maps and institutional affiliations.

Springer Nature or its licensor (e.g. a society or other partner) holds exclusive rights to this article under a publishing agreement with the author(s) or other rightsholder(s); author self-archiving of the accepted manuscript version of this article is solely governed by the terms of such publishing agreement and applicable law.